Journal Pre-proof

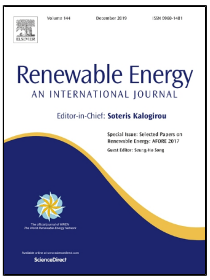

Modelling and experimental investigations of microcracks in crystalline silicon photovoltaics: A review

Lamprini Papargyri, Marios Theristis, Bernhard Kubicek, Thomas Krametz, Christoph Mayr, Panos Papanastasiou, George E. Georghiou

PII:	S0960-1481(19)31158-9
DOI:	https://doi.org/10.1016/j.renene.2019.07.138
Reference:	RENE 12050
To appear in:	*Renewable Energy*
Received Date:	18 February 2019
Accepted Date:	29 July 2019

Please cite this article as: Lamprini Papargyri, Marios Theristis, Bernhard Kubicek, Thomas Krametz, Christoph Mayr, Panos Papanastasiou, George E. Georghiou, Modelling and experimental investigations of microcracks in crystalline silicon photovoltaics: A review, *Renewable Energy* (2019), https://doi.org/10.1016/j.renene.2019.07.138

Modelling and experimental investigations of microcracks in crystalline silicon photovoltaics: A review

Lamprini Papargyri (corresponding author, papargyri.lamprini@ucy.ac.cy)

PV Technology Laboratory, FOSS Research Centre for Sustainable Energy, University of Cyprus, Nicosia, 1678, Cyprus

Department of Civil and Environmental Engineering, University of Cyprus, Nicosia 1678, Cyprus

Marios Theristis (theristis.marios@ucy.ac.cy)

PV Technology Laboratory, FOSS Research Centre for Sustainable Energy, Department of Electrical and Computer Engineering, University of Cyprus, Nicosia, 1678, Cyprus

Bernhard Kubicek (Bernhard.kubicek@ait.ac.at)

Austrian Institute of Technology, Vienna 1210, Austria

Thomas Krametz (Thomas.Krametz@ait.ac.at)

Austrian Institute of Technology, Vienna 1210, Austria

Christoph Mayr (Christoph.Mayr@ait.ac.at)

Austrian Institute of Technology, Vienna 1210, Austria

Panos Papanastasiou (panospap@ucy.ac.cy)

PV Technology Laboratory, FOSS Research Centre for Sustainable Energy, University of Cyprus, Nicosia, 1678, Cyprus

Department of Civil and Environmental Engineering, University of Cyprus, Nicosia 1678, Cyprus

George E. Georghiou (geg@ucy.ac.cy)

PV Technology Laboratory, FOSS Research Centre for Sustainable Energy, Department of Electrical and Computer Engineering, University of Cyprus, Nicosia, 1678, Cyprus

Modelling and experimental investigations of microcracks in crystalline silicon photovoltaics: A review

Lamprini Papargyri[1,2,*], Marios Theristis[1], Bernhard Kubicek[3], Thomas Krametz[3], Christoph Mayr[3], Panos Papanastasiou[1,2] and George E. Georghiou[1]

[1] *PV Technology Laboratory, FOSS Research Centre for Sustainable Energy, Department of Electrical and Computer Engineering, University of Cyprus, Nicosia 1678, Cyprus*

[2] *Department of Civil and Environmental Engineering, University of Cyprus, Nicosia 1678, Cyprus*

[3] *Austrian Institute of Technology, Vienna 1210, Austria*

**corresponding author email: papargyri.lamprini@ucy.ac.cy*

Abstract

In recent years, the scientific research into photovoltaic (PV) technology has focused on the failure modes in order to increase the PV reliability, durability and service lifetime. One of the predominant failure modes that appears in the crystalline silicon (c-Si) PV technology is the cell cracking that may damage the mechanical integrity of the PV module and hence, result in power loss due to the disconnected areas of the cell. Other forms of degradation may also be triggered such as potential induced degradation (PID) and hot spots. Therefore, the understanding of the cracking mechanism is of great importance. This paper presents the origins and factors that affect the cell cracks. Classification of cracks has been conducted as their characteristics determine the mechanical and electrical degradation of the PV module. Furthermore, experimental and numerical studies related to PV cracks on the scale of wafer, cell and PV module are analysed in detail. The results from the above investigations show that cracks do not always lead to a strong performance degradation and therefore the impact of cracks on the electrical characteristics of PV modules is still debatable.

Keywords: cracks, photovoltaics, reliability, degradation, fracture

Nomenclature

C_{ijkl}	Components of the fourth-order stiffness tensor of material properties or Elastic moduli (GPa)
E	Young's modulus (GPa)
EQE	External Quantum Efficiency (%)
G	Shear modulus (GPa)
I	Current (A)
I_{SC}	Short-circuit current (A)
J_{REV}	Reverse current density (A)
Lc	Critical length (mm)

m	Weibull modulus (-)
p	Pressure (MPa)
P_{MPP}	Maximum power output (W)
R_S	Series resistance (Ω)
R_{SH}	Shunt resistance (Ω)
t	Thickness (mm)
V_{MPP}	Voltage at maximum power (V)
V_{OC}	Open-circuit voltage (V)
y	Deflection (mm)

Greek letters

ΔP_{MPP}	Maximum power loss (%)
εij	Components of the strain tensor (-)
λ	Eigenvalue
v	Poisson's ratio (-)
σ_θ	Characteristic strength (MPa)
$\sigma_{applied}$	Applied stress (MPa)
σij	Components of the stress tensor (GPa)
σ_{max}	Maximum stress (MPa)

Abbreviations

Ag	Silver
Al	Aluminium
c-Si	Crystalline Silicon
CZM	Cohesive Zone Modelling
CTE	Coefficient of thermal expansion
DH	Damp Heat
DML	Dynamic mechanical load
DuraMat	Durable Module Materials
DWS	Diamond wire saw
EL	Electroluminescence
EVA	Ethylene Vinyl Acetate
FEA	Finite Element Analysis
FF	Fill Factor
IEA	International Energy Agency

ITRPV	International Technology Roadmap for Photovoltaics
LiT	Lock-in thermography
MBB	Multi-Busbar
ML	Mechanical loading
MPP	Maximum Power Point
OMA	Operational Modal Analysis
PVPS	Photovoltaic Power Systems
PL	Photoluminescence
PV	Photovoltaic
PVB	Polyvinylbutyral
Si	Silicon
SML	Static mechanical load
SUC	Small Unit Compounds
SWCT	Smartwire contacting technology
SWS	Slurry wire saw
TCT	Thermal cycling test
TPSE	Thermoplastic silicon elastomer
3D	Three dimensions
3PB	3 Point bending
4PB	4 Point bending

1. Introduction

The photovoltaic industry, with crystalline silicon (c-Si) as the most commonly used semiconducting material, is growing to meet global clean energy needs. The silicon (Si) wafer contributes about 40% to the cost of a silicon solar cell [1]. The 2010 International Technology Roadmap for Photovoltaics (ITRPV) reported that a large reduction in silicon solar cell wafer thickness was required to decrease the cost of solar cells and hence, of PV modules [1]. However, thinner wafers led to lower robustness of the solar cells against mechanical loads resulting in cell cracking. One of the present technological challenges is to identify and eliminate the sources of mechanical defects that may trigger crack initiation and propagation resulting in mechanical degradation of the wafer and ultimately in the breakage of silicon wafers and cells.

During cell fabrication, the solar cells are thermomechanically loaded and therefore permanent deformations are induced [2]. These permanent deformations correspond to significant residual stresses which can lead to cracking in the silicon solar cells. It was found that 2% of silicon wafers break during their production resulting in a yield reduction, rise in production cost and material losses of 5–10% [3]. Although optimising the fabrication processes may reduce cell cracking, imperfections during production are still unavoidable. The crack problem becomes worst as the wafer thickness is reduced [4], [5]. Due to this, even though all the damaged cells are detected and eliminated from the production process, it is

difficult to avoid completely the formation of microcracking and to quantify its long-term impact on the PV module performance. Existing imperfections and microcracks from production raise the breakage risk during the whole production cycle as they could further propagate by loads during the transportation, handling and installation in the field [6]. Crack formation and propagation may also take place during operation when wind loads, snow loads and temperature cycles are applied to PV modules [7].

Cracks are often invisible to the bare eye and could lead to electrically disconnected cell regions, causing a linear decrease in short-circuit current and higher series resistance, hence reducing the power output of a module [8], [9]. Furthermore, microcracks act primarily as recombination centres with a local temperature increase [10]–[12]. Overall, the length, orientation and position of microcracks in the Si wafer influence the output of multicrystalline (multi-c-Si) and mono-crystalline silicon (mono-c-Si) cells.

Often, mechanical loads induce cracks in wafer-based solar cells, which usually lead up to 2.5% power degradation in 60-cell PV modules, in the case the cracks do not isolate cell areas [8]. Furthermore, PV modules may exhibit cracks causing inactive cell areas after 15 years of operation. A survey of more than 250 PV modules reported power losses of up to 20% due to cell cracks in combination with ethylene vinyl acetate (EVA) browning and delamination [13]. Experimental results reported that cell cracking caused a power degradation of 4% and a reduced fill factor (*FF*) by 3% [14]. Results from another mechanical load test reported that the maximum output power (P_{MPP}) and *FF* were decreased by 3.6% and 3%, respectively [15]. After the application of 200 humidity freeze (HF) cycles, existing cracks propagated and expanded the electrically isolated regions causing up to 10% power degradation. Kilikevičius *et al.* [16] observed a power reduction of 1.37% after the application of dynamic loading which is acceptable considering the 3% limit. Kajari-Schröder *et al.* [16], found that 7% of the cracked cells had developed an inactive area and 29% of them had degraded after mechanical loading and 200 HF cycles. Morlier *et al.* [17] simulated the effect of cell cracks on PV module power output, considering the geometry of broken cells and the corresponding broken area. They have reported that up to 19% of the modules lost more than 20% of their power output. Observations suggest that if a crack that crosses a finger is open enough, the finger may fail in tension and the electric flow to the busbar will be blocked. It was observed that the number of cracks and power degradation cannot be correlated due to the different crack characteristics (e.g. direction, position, width etc) [18]. The power degradation due to these cracks increases with time and when the crack resistance reaches a value above 10 Ω inactive areas may develop as well [8], [17]. Because of the isolated cell region, the cell is driven into reverse bias and the full current flow along the localised path may lead to hot spots [19].

When the proportion of disconnected cell area is greater than 8%, the associated power loss is roughly proportional to the disconnected cell area whereas for series connected PV modules, the variation of power loss is super-linear. For typical 60-cell modules when the disconnected cell area reaches approximately 50% the bypass diode is activated causing loss of approximately one-third of the module power leading to module failure [18]. Even though, long-term power degradation due to cell cracking could become a crucial wear out mechanism, the knowledge and understanding of the phenomenon is still obscure and there is no well-defined set of tests that account for it in IEC 61215 [20].

Cracks in PV modules due to thermomechanical loads that may develop are being examined, since they may reduce the efficiency and reliability of PV modules [21]. The importance of further investigating this failure mechanism is evident by the increasing number of international activities and initiatives taken by the International Energy Agency (IEA) PV Power Systems Programme (PVPS), Sandia National Laboratories (SNL) and the National Renewable Energy Laboratory (NREL), to name a few. A report from IEA PVPS Task 13, characterised cracks as the dominant failure mechanism in the first two years of

operation causing a degradation rate of up to 3% per year at all climatic zones besides the cold and snow climate where it can reach 8% per year [22]. Furthermore, the Durable Module Materials (DuraMat) consortium is conducting research in the development of improved materials in order to mitigate cell cracks and other forms of degradation [23]. Although, there is a great interest towards the mitigation and better understanding of cracks in PV, there are no review studies available besides a few that are related to crack detection techniques only [21], [24]–[26]. While a considerable number of works regarding the initiation and effects of cracks in PV modules has been published, at the time of writing this paper, to the best of the authors' knowledge, none of the existing literature has conducted nor reported a comprehensive review on the topic of experimental and numerical simulations of cracks in PV modules. Knowledge on the simulation and experimental studies of PV cracks is very important in order to understand their full impact both on the mechanical and electrical degradation of the PV modules.

The present study analyses and identifies various aspects that can be useful to the research and industrial community in order to get an in-depth and systematic knowledge on the topic of PV microcracks. The information related to cracks in silicon wafers and PV modules is quite scattered in the literature; hence it is challenging to identify the cracks 1) origin, 2) root causes and factors that affect them, 3) classification in categories, 4) the way they propagate and 5) the simulations/experiments that have been performed so far regarding their effect on the mechanical and electrical characteristics of the PV module. Therefore, this work seeks to provide an overview, critically analysing and assessing the available studies reported in the literature, in order to provide a better understanding of the parameters that cause the formation and propagation of PV microcracks and their effect on the structural strength and power output.

2. Origin of microcracks

There are several stages related to the formation of microcracks: (i) the cutting process of an ingot or crystal bar, (ii) the cell or module production process due to external factors, (iii) improper module transportation/installation and (iv) the power plant operation period due to external environmental factors such as snow, wind etc [27]. The variation of production process can cause cracks during PV module production [18], which can be avoided by improving the production processes [28]. Wafer slicing, cell soldering and lamination processes during the fabrication of the Si cells and modules cause additional cracks and therefore the mechanical integrity of the structure will be reduced.

Most of the Si substrates in Photovoltaic applications are produced by casting a Si ingot succeeded by wafer sawing. Wire sawing [29], which is the first step of processing a Si ingot, leads to machining damages such as cracks in the surface or subsurface of the Si wafer. The diamond wire saw (DWS) wafering technology, which has been widely used during the last years, is less expensive than the conventional slurry wire saw (SWS) wafering technology. Although, DWS cut wafers cause a larger number of cracks compared to SWS cut wafers [30] whereas the subsurface crack depth induced by SWS is higher to the one induced by DWS [31], [32]. In the case of SWS, cracks have a typical depth between 10-20 μm [33] and their distribution is random [34]. Due to DWS, cracks can be found periodically along the direction of sawing [35] and the typical crack depth is 2-13 μm [35]. However, a correlation between the grain orientation and the crack depth is debatable [35], [36]. The failure strength of wafers along the wire direction is reduced compared to slurry-cut wafers, but increases in the direction perpendicular to the wire [37]. Watanabe *et al*. reported that the damaged layer thickness can be reduced from 20 to 8 μm if SWS is replaced by DWS [38]. Optimising parameters like the feed rate [31], grit size [39], speed [31], [35], [40], tension force, bow angles of wire saw [41] and the type of resin [38] may reduce the crack depth.

The higher the original subsurface microcrack depth is on the wafer surface, the easier the crack is formed. Therefore, material removal during sawing can be considered as many micro indentations that cause microcracks, rough surface and an electron-hole pairs recombination, requiring removal by saw damage etching process [42]. A number of studies reported that as-cut wafers are much less stable compared to etched wafers [43]–[45]. Moreover, though the etching process is expensive, it is intended to decrease the amount of damage or to avoid it completely.

One of the most vital processing steps during the production of screen-printed solar cells is the firing process, during which the screen-printed aluminium and silver paste are fired at high temperature in order to create electrical contacts [46], [47]. Due to mismatch of the thermomechanical properties of different materials, residual stresses are induced within the Si solar cell. Wafer bowing which occurs upon cooling, can be reduced by changing the amount and chemistry of paste and firing conditions [47]. Nevertheless, there is a limit below which screen-printed aluminium paste will lead to a non-uniform back surface field layer, influencing the electrical properties of the cell [48], [49].

In addition, the soldering process is a critical step in the fabrication of crystalline silicon PV modules especially during recent years, where the thickness of the wafers has been drastically reduced whereas the cell area has been increased. Due to the variance of coefficients of thermal expansion (CTE), large thermomechanical stresses are induced during the soldering process. These stresses can cause cracks which may grow when the PV module is exposed to thermal cycling. Cracks used to be frequently generated from the physical contact of brittle c-Si cells using electric iron heating for the soldering. Later on, infrared light [50]–[52] and laser heating technologies [53]–[55] have been introduced in order to avoid the physical contact and hence, any crack formation. With the technological progress, new interconnection methods have been applied in the PV industry such as ultrasonic heating [56], thermal spraying [57], conductive adhesives [58]–[63] and electromagnetic induction soldering [64].

The lamination (encapsulation) process is important for the integrity of PV modules whereas the focus is generally on the evaluation of the impact of the process on the encapsulation quality of PV modules. The relation of module reliability with encapsulation quality has not yet been adequately addressed in the literature [22]. Despite this, a significant number of failures has been reported during lamination showing high residual stress in the PV modules which tend to create cell cracks. Previous studies have reported that the maximum stresses are positioned close to the edge of the copper interconnector, and therefore cracks are expected to initiate in this area. Another experimental study showed that cracks due to lamination exhibit a ± 45° orientation [65]. Changing material properties like the encapsulant stiffness [66], [67] and the interconnect thickness [65] can reduce the propensity of cracking.

Besides the cracks caused during production, risks exist also during packaging and transportation of PV modules [68]. Currently there is no standard process on PV modules transportation. Only a few studies investigated the impact of transportation of PV modules on the cracking behaviour and hence, the PV power. Transport simulation tests showed that single cracks may appear in PV modules causing a power loss lower than 1% [6], [68]. Improper transportation and handling can be mitigated by redesigning the packaging with added protection and padding. It has been reported that transporting the modules vertically has a lower impact to cell cracks compared to horizontal stacked modules [6]. The stresses produced during handling and transportation, focusing on wafer handling method, called “Bernoulli gripping”, were examined in [69] which showed that the air flow rate, wafer type and thickness can influence the range and distribution of stresses produced in the wafer. Transport simulation of 3 hours produced single microcracks on the packaged modules which resulted in a maximum power loss of ΔP_{MPP}=-1.5%. [68]. Subsequently, the modules were exposed to different environmental tests such as thermal cycling and dynamic wind and

a maximum power loss of 2.8% was recorded. To determine the electrical and mechanical behaviour of the PV modules electroluminescence (EL) images were taken as well as IV-measurements.

Finally, PV modules are exposed to harsh outdoor conditions sometimes characterised by deep thermal cycles, high wind speeds [70], snow loading [8], [71], [72] and hail impacts [71], [73]–[75] that may cause permanent damage and/or power degradation during the system's lifetime. Such environmental conditions increase the stress beyond the residual stresses from the production processes such as lamination and soldering. Hence, extreme climatic conditions lead to higher fracture probability and reduce PV module reliability and efficiency [3–5]. Mechanical loads on PV modules can also be generated from snow and wind. With densities from 30-50 kg/m^3 (fresh snow) to 800-900 kg/m^3 (frozen snow), snow causes a heavy static load on the whole PV module which defined by the snow height [76]. An X-crack pattern can be observed in the case of a heavy homogenous ML such as snow [18]. Moreover, it should be noted that snow and ice under various circumstances may cause both uniform and partial shading and therefore it is crucial to examine the behaviour and influence of snow and ice on PV modules. Wind can act steadily and transiently, imposing static and dynamic loads on PV modules while hail causes an impact stress. Depending on the wind direction, cells may be under compression or tension. If the cells are under tension, cracks may be formed. However, when the load is withdrawn, cracks may close resulting to an electric recovery [77]. When hailstones act on a semi-flexible PV module, depending on their size and velocity, they can damage the front cover material or the active parts leading to a high local impact on the performance of the PV module. In the case of rigid PV modules, cell cracks depend on the glass thickness, hail characteristics (hail stone size and intensity, wind speed etc), mounting and frame type [71]. A glass-glass PV module can withstand the impact of hailstones without cell cracks [71]. The impact of hailstone was reproduced experimentally with impact tests using a pneumatic gun on semi-flexible PV and simulated numerically following two approaches in FEAP software by Corrado *et al.* [75]. It was shown that the plastic cover usually remains undamaged after the impact, while the solar cells exhibit cracks, whose extension depends on the substrate stiffness. Moreover, it was reported that the harder the substrate is, the more likely is that the damage will remain localised in a small region around the impact point, which becomes electrically inactive, whereas the outer area forms a few radial cracks, as it is depicted in Figure 1. When such loads act on a module, the solar cells bend depending on the structure of the glass, frame and mounting structures. Snow and wind loads are among the five most common causes of damage and account for 10-30% of failures [78].

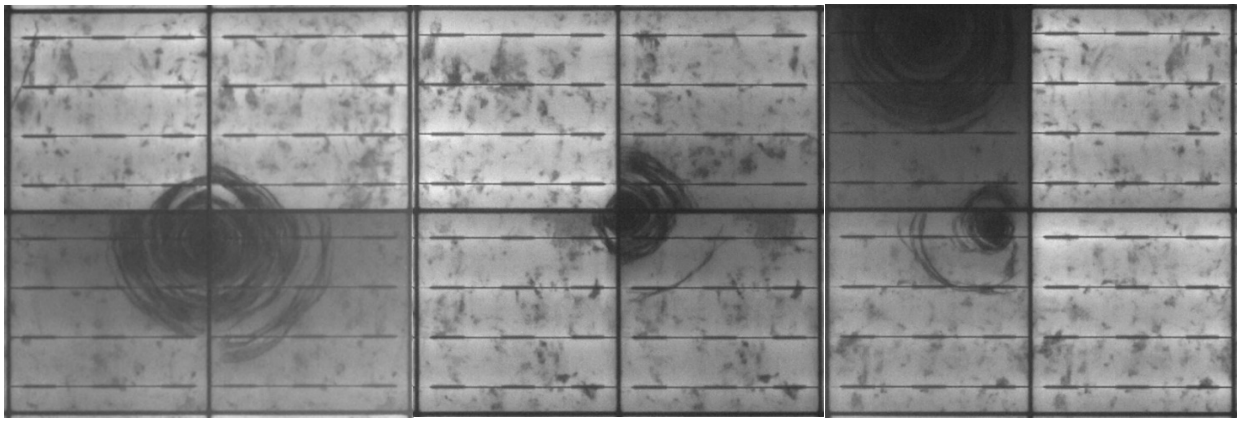

Figure 1. EL images showing the results of experimentally simulated hail impact obtained at Austrian Institute of Technology (AIT). Some radial cracks form around the impact point where the damage is located.

Although, cracks are unavoidable during either the production or the service life of PV modules, it is important to identify crack characteristics in order to mitigate crack formation and propagation. Crack characteristics such as critical points for crack formation, pattern, orientation etc. and parameters that affect them are strongly dependent on the stage that cracks were formed. Table 1 summarises the crack characteristics based on their origin.

214 **Table 1.** Summary of crack characteristics based on their origin.

Origin	How the cracks initiated	Crack distribution	Parameters that affect cracks	Comments
Slurry wire sawing (SWS)	Damage due to interaction between the cutting grits (SiC particles), the wire and the Si wafer [29].	Random crack distribution in Si wafers; typical crack depth, 10-20 μm [33].	The larger the grits the longer the cracks are [30].	The subsurface crack depth induced by SWS is greater compared to the one induced by DWS [30]–[32], [79]. The crack depth can be reduced from 20 to 8 μm if SWS is replaced by DWS [38]. DWS cut wafers cause a larger number of cracks compared to SWS cut wafers [30]. The failure strength of wafers along the wire direction in DWS is reduced compared to slurry-cut wafers, while it is increased in the direction perpendicular to the wire [37].
Diamond wire sawing (DWS)	Cracks occur due to scratching of the Si wafer by diamond grits [31].	Along the direction of sawing grooves and appear periodically in Si wafers [35]; the typical crack depth range between 2 μm and 13 μm [35]. Debatable correlation between the grain orientation and the crack depth [35], [36].	Decreasing feed rate [31], grit size [39] and increasing wire speed [31], [35], [40] may reduce the crack depth. Important to control the tension force and bow angles of wire saw to avoid any surface cracks [41]. The resin used as the bonding material of the grit on the wire could decrease cracks since it absorbs vibrations and shocks during the wire sawing process [38].	
Firing	Due to the thermomechanical stresses induced by the high temperatures of the electrical contact process [46], [47].	Initiate along the rear busbar in the interface between the Al and Al/Ag busbar [80] and propagate from the interface into the as-cut silicon wafer [46], [47].	Paste chemistry and firing conditions may reduce wafer bowing and residual stresses [47].	Screen-printing and firing could increase the number of cracked cells by about 1% due to repeated errors [81].
Soldering	Due to thermomechanical stresses in the cells because of the CTE variations of different materials [82].	The region near the end of the soldering path in Si layer is a critical area due to the higher thermomechanical stresses [83], [84]. Cell cracks initiate preferentially at the edge of the front busbar [85] having a diagonal or ± 45° orientation [86].	Increasing the speed and decreasing the power of the soldering system [84] and using a low solder melting point [87] reduce the probability of cracking.	The type of the interconnection technology affects the physical contact and therefore the mechanical stresses which are developed.
Lamination	The lamination process of Si cells creates residual stresses in the Si wafers due to high temperature and pressure [24].	Maximum stresses occur close to the edge of the copper interconnector [66], [88]–[91]. Cracks with a ± 45° orientation [65].	Higher encapsulant stiffness results to a lower fracture load [25], [31]. The stresses increase with thickening interconnects [30].	The lamination process is a critical operation in the production cycle because a number of new cracks occurs after this step [89]. The cells located near the frame experience more stresses and displacements [83].
Transportation	Due to vibrations and shocks [83].	Transport simulation tests exhibited single cell cracks distributed randomly along the module surface [6], [68].	PV stacking and transporting the modules vertically has a lower impact to cell cracks [33].	Transport simulation tests showed that cracks affect the power output marginally (power loss lower than 1%) [6], [68].

Snow	The weight of accumulated snow on the PV modules can cause fracture of the glass and Si cells [72].	Cell cracks with orientation parallel to the busbars and also diagonal and dendritic [18], [77]. An X-crack pattern is observed in the module level [18].	Applied load influenced by the snow density and height [76], e.g. . fresh snow of 1 m height applies 500 Pa [77]. Type of the adhesive between the frame and glass affects the durability of the module [71].	In order to simulate a homogenous snow or wind load, an SML test with a load of 2400 Pa is applied on horizontally mounted PV modules. A load of 5400 Pa is used to test the heavy load case [83]. Inclined PV modules which are installed in the field experience inhomogeneous snow loads with completely different load characteristics [92].
Wind	Wind pressure can increase the stress beyond the residual stresses leading to solar cells fracture [18].	The crack pattern similar to the case of snow loading [18].	When wind suction overpressure is applied, solar cells are at compressive stress and cracks are not formed [77]. If underpressure (in analogy to wind pressure or snow load) is applied the cells are under tension and cracks initiate/propagate.	Wind is assumed to be static in the IEC 61215 [20]. However, wind can act constantly or dynamically, imposing a static/dynamic mechanical load on the PV modules. Open cracks may close when the load is withdrawn resulting to an electric recovery [77]. Thus, PV modules in field can operate almost undisturbed after extreme events.
Hail	Due to hailstone impact, especially in semi-flexible PV modules [73].	Star cracks in rigid modules and star and radial cracks in semi-flexible modules [74], [75]. In semi-flexible PV modules with stiff substrate, cracks tend to concentrate near the impact point and an electrically insulated area may be generated. In a soft substrate, a much wider crack pattern occurs but most of the cracks are still electrically conductive [75].	In the case of rigid PV, cell cracks depend on the glass thickness, hail characteristics (hail stone size and intensity, wind speed etc.), mounting and frame type [71]. For semi-flexible PV, the crack pattern depends on the impact size and velocity and on the substrate stiffness [75].	A glass-glass PV module can withstand the impact of hailstones without cell cracks [71]. The impact of hailstones is examined in the IEC 61215. During this test, ice balls with a minimum diameter of 25 mm and a minimum velocity of 23 m/s are propelled on the PV module through a pneumatic launcher [20].

3. Classification of cracks

Cracks can be classified based on their size, shape, position, direction [93] and severity [8]. There are many shapes and sizes of microcracks within a Si cell based on how they are created. A line-shaped crack is caused by scratches and it commonly initiates due to wafer sawing or laser cutting [94]. Star-shaped cracks are initiated due to a point impact which induces several line cracks with a tendency to cross each other [95].

Cracks can be categorised as either macro or microcracks (μ-cracks) based on their width size. A crack with a width lower than 30 μm is referred to as a microcrack [21]. Cracks can also be classified based on their position. According to the literature, cracks that take place on the surface of a silicon wafer are known as facial or visible or edge cracks [96]. Cracks that are located below the wafer surface or are initiated on the surface and propagate in the depth direction are known as subfacial or invisible or interior cracks. Facial cracks which are usually created due to direct impact loading on the wafer edges [97], influence significantly the fracture strength during twist testing [98]. A facial crack with a length of 2 mm almost always leads to fracture in a mechanical twist test, but a subfacial crack with the same length may pass the test [96]. The classification scheme is shown in Figure 2.

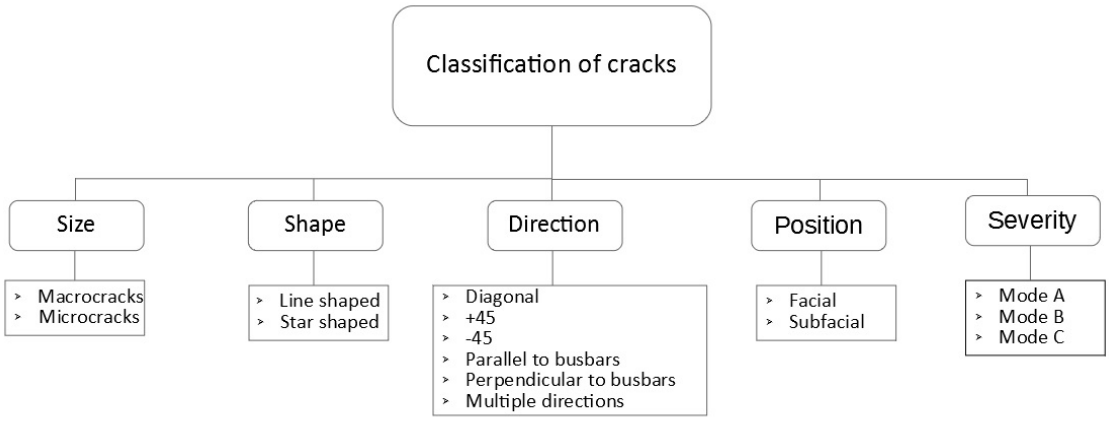

Figure 2. Classification of cracks according to their size, shape, direction, position and severity.

In terms of the crack direction, there are various types of cracks that might form in Si cells: diagonal cracks, parallel to busbars, perpendicular to busbars, +45°, -45° and multiple directions cracks. The classification of cell cracks based on their orientation is show in Figure 3. A significant power degradation was observed in the case of diagonal and multiple direction cracks [99].

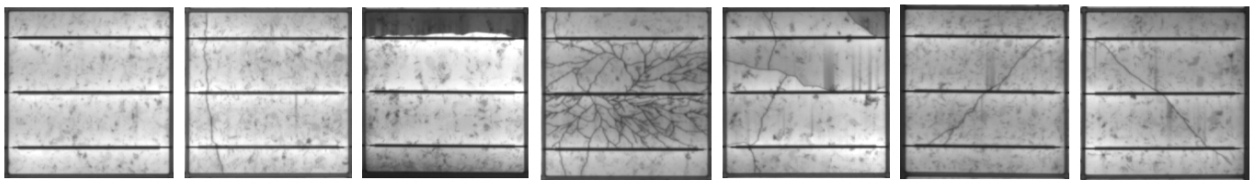

Figure 3. Classification of cracks based on their orientations in silicon solar cells. Types of cell crack from left to right: no crack, perpendicular, parallel, dendritic, multiple directions, +45°, -45° (images obtained from the Austrian Institute of Technology).

Cracks can be classified based on their severity as mode A, B and C (see also Figure 4). Cracks defined as mode A [8] do not introduce disconnected cell areas and do not show dark regions in EL images. Therefore, mode A cracks do not cause significant power loss. On the contrary, some regions of the affected Si cells may fracture and become partially (mode B crack) or completely (mode C crack) isolated from the rest electrical circuit, causing power degradation and in some cases leading to reverse bias of the Si cells forming hot spots [100]. Type B cracks show darker regions in high current EL images but the dark areas disappear in low current EL images, revealing that there is still electrical connection at the crack locations. Type C cracks are created when some areas are completely electrically isolated from the rest electrical circuit and they appear dark in EL images.

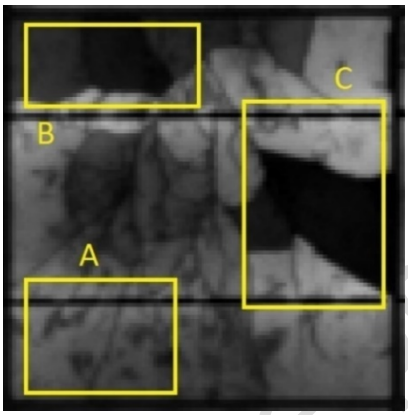

Figure 4. Electroluminescence image illustrating crack modes A, B and C (picture obtained from the PV Technology Laboratory of the University of Cyprus).

4. Influence of mechanical properties on cell cracks

In order to improve the reliability of PV modules, it is important to investigate the factors that lead to the initiation and propagation of cracks since they may cause a significant decrease in the PV power output [1,2]. One of the major factors affecting cell cracks are the mechanical properties of the PV module materials. The assessment of the mechanical properties is of paramount importance, since material stiffness and strength depend on the fabrication process.

4.1. Properties of silicon

Silicon is brittle at room temperature and therefore vulnerable to the defects such as cracks. Consequently, close to these defects, the stresses could be much higher than the macroscopic stress applied to a sample and the value $\sigma_{max}/\sigma_{applied}$ reaches infinity for a crack. Due to the brittleness of silicon, the stress at the crack tip cannot be released and if the stress exceeds the critical stress, the crack will propagate [102]. The conditions for crack propagation depend on stress concentration in the crack tip area and on macroscopic factors such as the geometry and dimensions of the sample [103]. Nevertheless, crack propagation is completely determined by atomic-scale phenomena [104], [105].

It is known that the cracks occur on the {1 1 0} [21], [106], [107] and {1 1 1} crystallographic planes [93], [108]–[110], as it was studied via simulations [93], [109], [111] and experimentally [109], [110], [112], [113]. Some researchers used Finite Element Analysis (FEA), molecular dynamics and quantum mechanics methods to develop models to determine the direction and speed of cracks in mono-c-Si wafer [114]–[117]. Miller indices which is a notation system for planes in crystal is depicted in Figure 5.

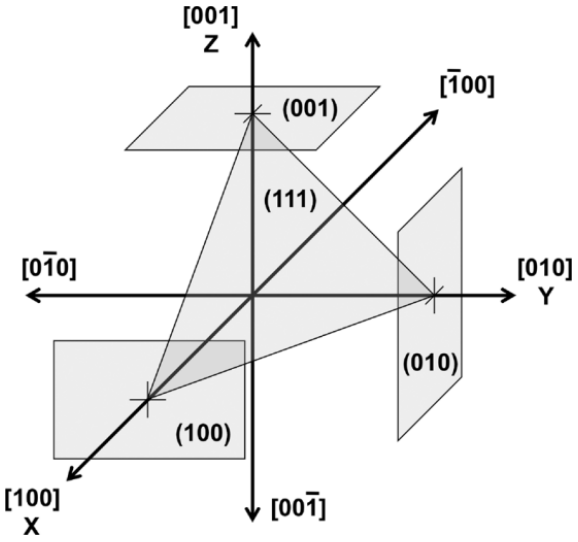

Figure 5. Miller indices in a cubic crystal. The directions [1 0 0], [0 1 0], and [0 0 1] are the XYZ Cartesian axes unless otherwise specified [118].

Silicon is an anisotropic material and its properties are strongly dependent on the crystals orientation [118]. In an anisotropic material, Hooke's law involves a fourth rank tensor to describe the elastic relationship between the stress σ and strain ε tensors in terms of stiffness C.

$$\sigma_{ij} = C_{ijkl}\varepsilon_{ij} \tag{1}$$

Monocrystalline silicon is characterised by three independent parameters due to the cubic symmetry of atoms in the crystal [9,13]. The most accurate values in the literature for the constitutive tensor along the [1 0 0] plane were reported by Hall [120], as presented below:

$$C^{100} = \begin{bmatrix} 165.7 & 63.9 & 63.9 \\ 63.9 & 165.7 & 63.9 \\ 63.9 & 63.9 & 165.7 \\ 0 & 0 & 0 \\ 0 & 0 & 0 \\ 0 & 0 & 0 \end{bmatrix} \tag{2}$$

283

284 In the case of isotropic material, stiffness C can be represented by a single value for Young's Modulus
285 E which characterises the stiffness of an elastic material and is calculated from the stress–strain curve elastic
286 slope. For orthotropic materials, such as silicon, the elastic properties can be determined from the Young's
287 modulus E, the Poisson's ratio v, and the shear modulus G [119]. The maximum value of Young's modulus
288 for mono-c-Si is 187.8 GPa and occurs in the [1 1 1] crystalline direction, while the minimum value of the
289 Young's modulus is 130.1 GPa and takes place in the [1 0 0] direction. The Eigenvalues and the Young's
290 modulus for [1 0 0], [11 0] and [1 1 1] which were computed in [121] are given in Table 2.

Table 2. Eigenvalues of the constitutive tensor and Young's Modulus, E, based on the crystalline directions.

Direction	λ_1 (GPa)	λ_2 (GPa)	λ_3 (GPa)	E (GPa)
[100]	180.3	101.8	79.6	130.1
[110]	226.3	143.6	62.1	169.1
[111]	194.4	146.8	57.1	187.8

The fracture of a multi-c-Si may occur due to transgranular and/or intergranular cracking. The grain orientations influence the stiffness of multi-c-Si and the Young's Modulus is 130.1- 187.8 GPa. If the sample dimensions are much higher than the grain size, the multi-c-Si can be considered as an isotropic material with only two elastic constants, e.g. E and v.

Temperature also influences the mechanical properties of Si [8,9]. At room temperature, Si behaves elastically and there is no plastic deformation [123]. Both mono-c-Si and multi-c-Si are brittle at ambient temperatures and present a brittle-ductile transition at temperatures near 600°C [124].

4.2. Expansion and contraction of materials

The most ordinary PV module consists of a glass, a polymeric encapsulant surrounding the silicon solar cells and a polymeric backsheet. Fingers which are very thin conductors, collect the generated electrons from the cell surface to the busbars (see Figure 6).

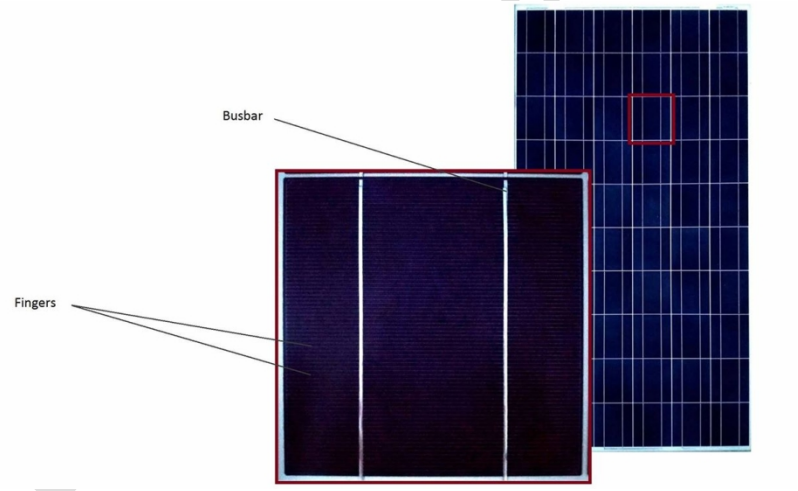

Figure 6. Sketch of a PV module and a Si cell showing the busbars and fingers over a silicon solar cell (Picture obtained from the PV Technology Laboratory of the University of Cyprus).

During production and operation, the materials which make up the PV module expand and contract due to the mismatch of their *CTE* [125]. Table 3 compares the *CTE* values for materials used in a PV module. This *CTE* variance of the bonded materials causes the thermomechanical induced deformation of the PV module. Thermal stresses occur whenever there is a change in temperature of the PV module, starting from the production processes and continuing to the daily and annual temperature cycles. The proper selection of encapsulant can reduce broken interconnectors and cell cracks [125]–[127].

Table 3. List of *CTE* values for materials used in a PV module.

Material	*CTE* (10^{-6}/K)	Reference
Glass	8	[91], [128]–[130]
EVA	270	[91], [128], [129]
Silicon	1.72 (T = 220 K) 2.23 (T = 260 K) 2.61 (T = 300 K) 2.92 (T = 340 K) 3.34 (T = 420 K)	[91], [128], [131]
Backsheet	50.4 88	[129] [72], [91]
Aluminium	23.1-23.9	[72] [84], [132], [133]
Solder	21-23.5	[84], [128], [132]
Copper	16.5-17	[64], [82], [84], [132]–[134]
Silver	9.8	[135]

4.3. Type of backsheet

A critical part of the photovoltaic structure is the backsheet whose role is to address and mitigate the environmental stresses and offer reliability to PV modules [136]. Experimental results have shown that the power loss of a PV laminate with backsheet was up to 2.2% while PV laminates without backsheet lost 10.3% of the initial power [137]. Moreover, Haase *et al.* [138] reported that the existence of backsheet reduced the crack width by 30% than in cases that there was no backsheet. In typical PV modules, a polymer is used as a backsheet material, but there are some cases that glass is preferred, as it is depicted in Figure 7. If a module with a polymer backsheet is loaded from the front side then the cells will be in the tensile zone and therefore they will experience large stress. But in the case that a glass is used as backsheet the whole structure is stiffer and deflects less for a given load [139], [140]. Consequently, the cells will be in neutral axis and the effect of loading will be much less. Although glass-on-glass PV module design offers higher reliability and longer durability compared to the traditional polymer design, considerations regarding the weight and safety issues should be taken into account [141].

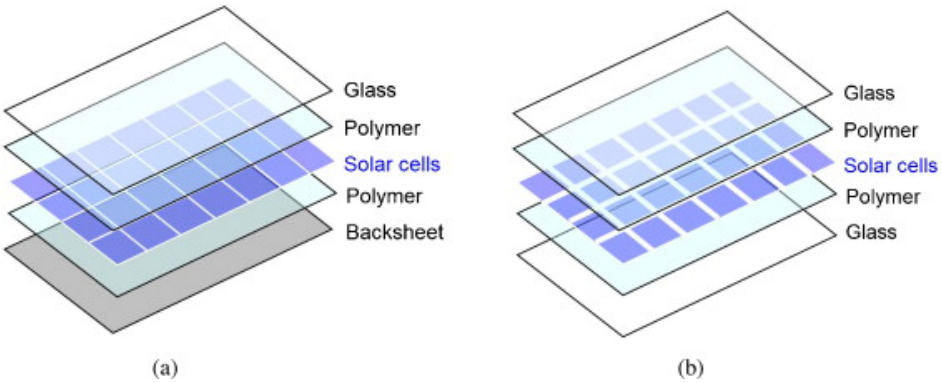

Figure 7. Two typical stacks of PV modules: a) Framed PV module with a polymer backsheet and b) a glass-on-glass PV module [142].

4.4. Type of encapsulant material

Polymer is commonly used to encapsulate the silicon solar cells and protect them from environmental influences such as mechanical loads or humidity and to reduce thermomechanical stresses from the difference of the CTE between glass-silicon and silicon-backsheet. Materials like Ethylene Vinyl acetate (EVA), Polyvinylbutyral (PVB), Polyethylene (PO) or Thermoplastic silicon elastomer (TPSE) are common polymers that are used for embedding solar cells [143]. EVA is the most common encapsulate material in the PV industry because it shows good weathering resistance, electrical and mechanical properties [2], [125]. The encapsulant stiffness which is dependent on temperature is a key factor that determines the strains that will be transferred from the glass to silicon solar cells [66].

The fracture strength strongly depends on the Young's modulus and thickness of the encapsulant [67], [144]. Dietrich *et al*. [19] reported that there is an interdependency between the type and the thickness of encapsulant in terms of the load that is applied to the solar cells. The combinations of stiff-thin and soft-thick encapsulants are those which increase the reliability. Rowell *et al.* [145] performed mechanical load and TC tests and reported that fracture load can be increased by 80% when the encapsulant thickness is double. Moreover, it was reported that fracture strength decreases with increasing Young's modulus. Sander *et al*. [52] experimentally characterised the in-plane fracture strength of a PV module equipped with two EVA encapsulation materials of different stiffness properties. The results proved that stiffer EVA induces cell cracks on the PV module at lower load. The influence of encapsulation stiffness at cold environmental conditions on fracture propensity within PV module was studied in [144].

5. Influence of the geometrical properties of the module on cell cracks

Another factor that affects the formation of cell cracks is the geometry of the corresponding module. The thickness and the position of each material in the PV module is crucial for the reliability of the structure.

5.1. Asymmetry of PV module

The glass is much thicker than the layer stack of the solar cell, the encapsulating material and the backsheet. Therefore, there is an asymmetric buildup/setting. The typical thicknesses of the PV module materials based on values that are found in the literature are listed in the Table 4 [146].

Table 4. Typical thickness of the materials that consist a PV module.

Material	Typical thickness (μm)
Glass	2000-4000
EVA	350-500
Silicon	120-200
Backsheet	250-400

The neutral plane, where the normal stresses on a cross-section are zero, is always positioned in the glass, which makes 70% of the module thickness, as qualitatively shown in Figure 8. If the PV modules are loaded from the front side EVA, cells and backsheet are located in the tensile zone. If the cell stress is higher than the tensile strength, the cells crack [5]. While under tensile stress, cell cracks tend to widen, affecting the conducting properties of the device. This can lead to the isolation of cell regions. However, once the tensile stress is removed, the cracks revert to the near closed state and the conductive properties are reinstated. This so called crack "healing" has been reported by Paggi *et al*. [101]. Although the trend is clear that as the front side pressure is reduced then more cracks close, sometimes effect is relatively random.

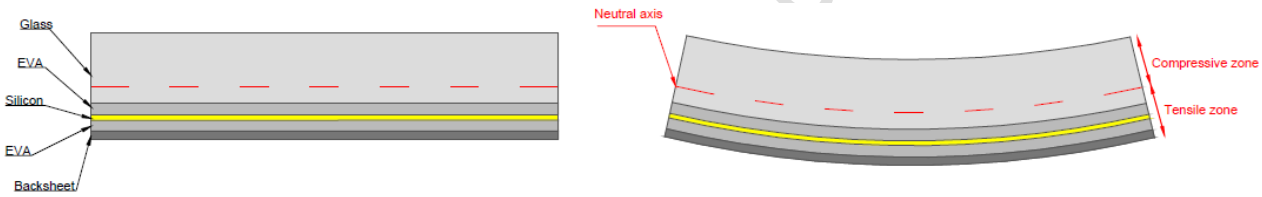

Figure 8. Layer structure of a standard PV module (left). If the PV module is loaded from the front side (top), silicon solar cells are always in the tensile zone and they tend to stretch (right).

5.2. Thickness of silicon

The demand to reduce PV production costs and the shortage of Si are leading to a reduction in wafer thickness. During recent years, the wafer thickness has decreased from about 300 to 150 μm and the cells have become more vulnerable to mechanical damages [147]. More recently wafer with a thickness of 100 μm has been used [148]. Thickness reduction without consequent adaptation of all steps in processing leads to a lower breakage force on cell level and thereby in increasing breakage rates and decreasing mechanical integrity of the PV module. Wafer thickness reduction leads to lower manufacturing yields and consequently to higher sensitivity of the solar cell to mechanical loads [4], [149]. Moreover, microcracks are less likely to propagate in thicker wafers. According to the linear fracture mechanics theory, under the same bending force the critical crack length L_c is proportional to the fourth power of the wafer thickness t [150].

5.3. Type of interconnection technology

Over the past few years, various interconnection technologies have been developed in order to achieve high reliability, minimise the shading events, reduce the series resistance and the silver paste consumption.

One approach is the dash-line cell busbar design which can be used instead of the traditional full-line pattern, reducing the silver paste which is used [151]. There are many types of dash-line busbars, such as 3,5,6 and 8-dash busbars. Although dash-line design can reach the high cell efficiency targets, the reliability of the module is under question. Chen *et al.* [152] reported that the potential risk of crack formation and power loss is increased with increasing the dash number of busbar pattern.

The Multi-Busbar (MBB) technology appears as another novel cell interconnection technology to increase the module power [153], [154]. In MBB technology 12-15 busbars [155]–[157] are used, instead of ribbon-based interconnection with 3-5 busbars [158]. As the number of the busbars increases, the requirement for lateral transport is reduced which results in lower series resistance [159]. At the same time, an increased number of busbars leads to the reduction of the area that could be isolated at the edges of the cells due to cracks [5]. Walter *et al.* [160] reported a superior mechanical behaviour in accelerated ageing for Multi Busbar (MBB) interconnection compared to the typical 3 busbar (3BB) interconnection technology.

Another approach is wire bonding technology which is known as SmartWire Contacting Technology (SWCT) and is applied to cells with front metallization and is consisted only of copper wires (no busbars are used) [161], [162]. This technology requires the combination of lamination and interconnection into a single lamination step whose temperature is kept below 160 °C and therefore the probability of wafer fracture is less compared to the traditional production processing steps [163]. Moreover, SWCT reduces the impact of cell breakage because of the increased number of current collection paths [164].

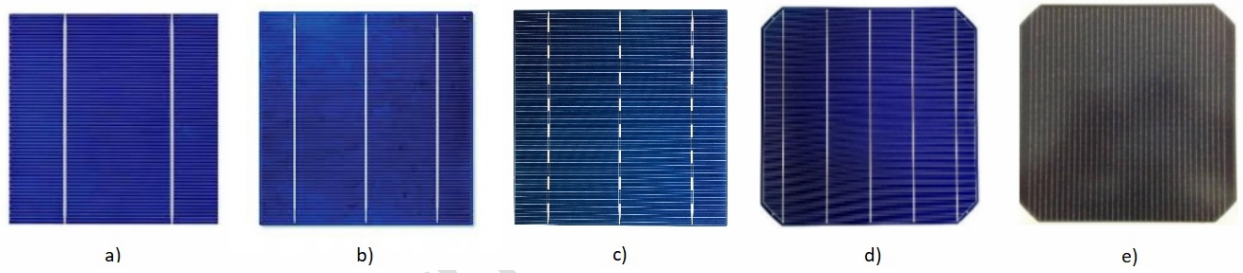

Figure 9. Different interconnection technologies. a) 2BB b) 3BB c) 3BB with dash-line pattern d) 5BB e) multiwire with no busbars.

5.4. Frame and backrails support

Stiffer frames and/or frames with additional stiffening elements such as backrails perform better than conventional PV structures [165], [166]. Although extra support stiffens the module and effectively reduces the deflection, it increases the material and shipping costs. The mechanical rigidity is determined by the amount, the cross section and the orientation of the supporting elements. In order to increase the stiffness of the module, Nussbaumer *et al*. [167] proposed a rigid structure for the rear side of the module or a subdivision of the module in smaller parts. The latter structure which is known as Small Unit Compounds (SUC) module can also be used for the mounting of the module. Beinert *et al.* [146] performed mechanical load tests on PV modules with and without frame and reported that the existence of frame increases the fracture strength and reduces the probability of crack formation.

The stiffness of a typical c-Si module depends on the frame and the front glass. Reducing the dimensions and weight of either frame or glass leads to a lower mechanical integrity of the structure. Standard glass/backsheet modules with circumferential frame have a large unsupported central laminate area, which may result in a damage of the module [167]. Glass-on-glass structures are very stiff and show almost no

deflection. Therefore, they may be mounted without an additional frame if the thicknesses and/or the Young's Modulus of the glasses are sufficient.

6. Modelling microcracks in PV modules

Modelling and simulation of cracks in PV modules can provide additional insights that are often impossible to discover through experimental and theoretical analysis alone. Many researchers have implemented Finite Element Analysis (FEA) to simulate the stresses and deflections of PV modules during the production and also during operation. Some studies have focused on the simulation of the thermomechanical stresses that are induced in the PV module during production or in the field and others investigated the effect of cracking on the electrical characteristics of the PV module.

6.1. Simulation of stresses during production

Rigorous research and development strategy is required for the optimization of the parameters involved in the production of the PV modules in order to improve their reliability. The application of FEA in the design of PV modules has the potential to identify issues with potential residual stresses from soldering and lamination processes and the response of the structure to static and dynamic thermomechanical stresses and strains. The above techniques could be used to optimise parameter settings for control factors in the module assembly line, enabling the identification of optimal parameter settings for improved durability of PV modules. The wafer breakage during fabrication depends on structural defects such as cracks, the stress applied to the wafer during processing and the residual stress developed in the wafer in prior processing steps and defects such as cracks [69].

There have been many studies that investigated the residual stresses from the soldering process, however these studies failed to consider the post-lamination stresses. Gabor *et al*. [82] showed that soldering induced damage is caused by the different CTE of copper and silicon and it leads to the initiation and/or propagation of cracks. Kraemer *et al*. [85] developed a 3D FEA model and analysed the post-soldering thermomechanical stresses generated in the cells. Stresses were induced when the solder solidifies and cools down to room temperature. The FEA simulation results showed high compressive stress in the Si below the copper interconnections due to the higher CTE of the copper ribbons. These results indicated that first cracks may appear at the very edge of the solder layer. Dietrich *et al*. [168] used FEA simulations and bending tests on PV modules to study the impact of different metallization structures on cell stress. The results showed that not taking into account the soldering induced stresses results in incomplete fracture assessment of Si cells. Nasr Esfahani *et al*. [84] developed a FE model to simulate the soldering process of a Si cell in order to study the distribution of temperature and stresses in cell materials. The findings conclude that the final points in the soldering path of the Si layer can be considered as a critical area due to the higher thermomechanical stresses. Xiong *et al*. [64] investigated the initiation and orientational distribution of cracks induced by electromagnetic induction soldering. The number of cracked cells was recorded and different types of cracks were analysed. Chen *et al*. [132] simulated the residual stresses and bow of the cell due to soldering and showed that thinner cells crack due to high stress during soldering. Wiese *et al*. [169] investigated the impact of Young's Modulus, yield stress, and the dimensions of the copper wire on the principal stresses induced in silicon layer during the production process. The findings indicated that increasing the Young's Modulus and the yield stress creates higher stresses in the silicon wafer. Lai *et al*. [133] pointed out that the maximum stress developed in the Si layer during the soldering process occurs where the wire and silicon meet. Moreover, they reported that as the wafer thickness and the aspect ratio of soldering rod reduce, the residual stress increases.

Many researchers have computed the post lamination thermomechanical stresses in PV modules without taking into account the residual post-soldering stresses. Lee and Tay [72] performed 3D FEA simulations of a PV laminate to compute the post lamination thermomechanical stresses. Then they computed the stress redistributions within the laminate when it is framed, installed, and exposed to a 5400 Pa uniform load. They found that the largest maximum principal stresses take place at the edges of the glass-frame which may cause glass to fracture. The cells are under tension, but this is not critical as the stresses are much lower than failure stress of the silicon cells. Zhang *et al*. [88] also implemented similar simulations of post lamination cooling process in order to find the residual stress in the PV laminate. Although they used the sub modelling method to include the soldered copper interconnects in their investigation, the actual post-soldering stresses in the laminate could not be represented since they assumed that the initial stress at the lamination temperature in the laminate was zero. The findings show that the maximum cell stresses are positioned close to the copper interconnects, which means that the cracks and the delamination of the solder ribbon most possibly occur near the interconnection ribbon, which was verified experimentally [89], [90]. Sun *et al*. [170] used analytical modelling to compute stresses due to lamination and thermal loading but this model did not take into account cell stress/bow due to soldering.

The residual stress in a PV laminate is the result of the accumulation of residual stresses from each production process. Dietrich *et al*. [171] computed the lamination and post lamination cooling stresses and then they used a linear superposition with post soldering stresses to calculate the accumulated cell stresses in the laminate. The use of linear superposition is questionable, due to the plastic deformation of solder and copper. The post-soldering, lamination and post-lamination cooling stresses were numerically simulated and experimentally validated in [128]. Song *et al*. [91] simulated the evolution of stresses in Si cells of a PV laminate following the different manufacturing steps of the soldering of interconnect ribbons onto wafer cells, lamination, and post lamination cooling. It was observed that the highest stress in the modified PV laminate production cycle was the stress during the lamination and the majority of cracks is positioned along the cell close to the edge of the copper interconnects. Moreover, they reported that the final accumulated residual stresses that includes the post soldering, lamination, and post lamination thermal stress has been found to be about 20% higher than what was reported elsewhere [88], [172]. Li *et al.* [83] performed FEA to study the thermomechanical behaviour of SWCT and busbar PV modules during production, transportation, and subsequent thermomechanical loads in a consecutive step-by-step manner. The results showed that higher stresses are induced in case of busbar PV compared to SWCT interconnection and the critical area for fracture is close to the busbar edges. Table 5 shows a list of numerical studies that evaluate the residual thermomechanical stresses due to soldering, lamination, and operational loads with main results and remarks. An extensive summary of several numerical models reported in the literature is given in Table 4. From this Table it is obvious that different models were applied at different stages of the production line. It is also notable that the majority of these models are not validated experimentally.

498 **Table 5.** A summary of numerical models that evaluate the residual thermal stress due to soldering,
499 lamination and other stresses due to operational loads.

	Residual stresses during						
Reference	Firing	Post soldering	Lamination	Post lamination-cooling	Stresses from load	Validation	Remarks
Lai *et al.* [133]	-	✓	-	-	-	-	Crack was introduced in the model. The residual stress of the cell increases as the cell thickness is reduced.
van Amstel *et al.* [173]	✓	-	-	-	-	✓	No cracks were observed.
Gabor *et al.* [82]	✓	✓	-	-	✓	✓	The residual stresses may cause cell cracks or fracture due to propagation of existing cracks.
Chen *et al.* [132]	-	✓	-	-	-	-	No crack was observed. The increasing residual stress may cause the damage in the region of wafer near electrode.
Dietrich *et al* [171]	-	✓	-	-	✓	✓	Neglecting intrinsic stresses induced by soldering leads to incomplete interpretations of the fracture characteristics and fracture rate of encapsulated solar cells.
El Esfahani *et al.* [84]	-	✓	-	-	-	-	The points between solder and Si can be considered as the critical area due to their higher temperature and thermomechanical stresses
Wiese *et al.* [169]	-	✓	-	-	-	-	No cracks were observed.
Song *et al.* [91]	-	✓	✓	✓	-	✓	The majority of cracks is positioned along the cell adjacent to the edge of the copper interconnects.
Kraemer *et al.* [85]	-	✓	-	-	-	-	The first cracks may appear at the very edge of the solder layer.
Zhang *et al.* [88]	-	-	-	✓	-	-	The cell cracks and the delamination of the solder ribbon most possibly take place near the interconnection ribbon.
Lee & Tay *et al.* [72]	-	-	-	✓	✓	-	Under testing, cells experience non critical tensile stresses as the failure stress of the silicon is not approached.
Tippabhotla *et al.* [128]	-	✓	✓	✓	-	✓	No cracks were observed.
Li *et al.* [83]	-	✓	✓	✓	✓	-	The regions close to busbar edges are crack sensitive points.

500

501 ### 6.2. Simulation of the stresses during operation

502 Weiss *et al*. [70] studied the dynamic deflections of PV modules in indoor and outdoor test conditions
503 and compared the results with the results of the FEA simulation. The outdoor measurement set up consisted
504 of an ultrasonic anemometer to measure the wind velocity and a laser distance sensor to measure the
505 deflection on the middle point of the PV module's backside. Although a direct correlation between the wind
506 velocity and the module deflection could not be determined in the field, a correlation between pressure and
507 module deflection could be measured in the lab. The correlation between the pressure p onto the module
508 and deflection y between -10 and +10 mm can be described as:

$$p = -62.689y - 0.21895y^2 - 0.1127y^3 \quad (3)$$

Dong *et al*. [174] presented a numerical simulation based on the mechanical behaviour of an ultra-thin double-glazing PV module under static and dynamic load conditions. Static, modal and mode-based steady-state dynamic analyses were conducted based on FEA for the three most commonly used mounting configurations (four edges fixed, six clamps fixed, four corners fixed). It was shown that the mounting configurations impact both the static (strength and deformation) and dynamic performance (dynamic characteristics and responses). Moreover, the observed deformations and stresses were large enough to cause cracks or fractures in the solar cell layer, or even damage of the whole PV module. Kilikevičius *et al*. [175] performed a FEA analysis which was validated experimentally in order to evaluate the possible resonant frequencies of PV modules and their reaction in different weather conditions. Five resonant frequencies and their corresponding displacement points were determined while the PV modules were fixed perimetrically. During the experiment, a PV module was subjected to cyclic mechanical loading and an Operational Modal Analysis (OMA) was used to identify the modal properties of the module. Changes on the frequency of oscillation and vibration amplitude (0-40 Hz) allow to simulate the dynamic mechanical loads which correspond to all possible severe weather conditions like wind or snow. The experimental results showed that a number of cracks was formed resulting in a power reduction of 1.37%.

6.3. Propagation of cracks and electric response

A computational model for the simulation of intergranular and transgranular cracking in multi-c-Si cells was developed by Infuso *et al.* [142]. A pre-processor and an image analysis method were used to create a FE mesh with embedded interface elements and a modified Cohesive Zone Modelling (CZM) approach was implemented to avoid mesh dependency. Another approach presented by Paggi and Reinoso [176] was able to combine both fracture modes and simulate complex crack patterns in anisotropic multi-c-Si microstructures with and without initial defects [121]. The phase field approach was used for transgranular cracking and the CZM for intergranular failure. Different values of the the fracture toughness of the grain boundaries to the fracture toughness of the grains were used in isotropic and anisotropic models in order to identify the crack pattern in each case.

In another study and under the assumption of a worst case scenario, cracks have been considered as defects interrupting fingers and leading to disconnected areas of a Si solar cell [8]. In that model, the position and direction of cracks with respect to the busbars were found to be key parameters, since they affect the electrical performance in different ways in relation to the insulated area of the Si cell. Based on the above simplification in which all cracks are insulating and therefore they behave as mode C , a multi-scale and multi-physics computational model for a PV laminate, based on nonlinear fracture mechanics cohesive zone model for simulating cracking in multi-c-Si has been developed in [177]. The model combined the electric and elastic fields and considered the grain boundaries as a source of microcracking. An advancement of the previous model was proposed by Paggi *et al.* [178] which included a more accurate electric model for each finger with localised resistances dependent on the crack opening and estimated the effect of microcracks and power degradation in PV modules based on a global–local multi-physics multi-scale approach. A thermoelastic CZM to simulate thermomechanical problems in Si cells during post lamination cooling, considering partial heat conduction across crack faced, depending on their opening was proposed by Sapora and Paggi [179]. Berardone *et al*. [180] generalised the one-dimensional model of Breitenstein and Rissland [181], to simulate the electric current distribution in Si cells accounting for a distributed series resistance to the presence of partially conductive cracks. In mono-c-Si cells, the impact

of crack opening on the electric response is clear, due to the increase in critical resistance by bending the module. However, in the case of multi-c-Si, the presence of defects, grain boundaries and imperfections make the model more complex and the results are ambiguous.

7. Experimental investigations on PV module microcracks

A limited number of studies is available related to the outdoor exposure and measurement techniques of microcracks. As mentioned earlier, cell cracking is the dominant failure mechanism in the first two years of operation with degradation rates of up to 3% per year [22]. Previous research studies showed that the electrical degradation due to cell cracks depends on the climate characteristics of the location that the PV modules are installed [22]. The power loss caused by cell cracks in the cold and snow climate is about 3% per year higher than in the moderate climate and 6% per year higher compared to the hot and dry climate. Sander *et al*. [52] reported that after a 4-month outdoor exposure no significant change in the characteristic strength could be measured. The above findings agree with another study where 20 PV modules were power rated in the lab after outdoor exposure and none of them showed a significant power loss and no additional crack was introduced or an existing crack expanded during the 6-month outdoor exposure [175]. Moreover, Buerhop *et al.* [182] exposed outdoors 54 pre-cracked modules (some of them were artificially stressed) for a 1 year period. Although no changes were observed in the electrical characteristics and in EL images after the outdoor exposure, the accelerated static load tests pointed out that above a certain limit, cracks develop. Wohlgemuth and Cunningham [183] reported that cell breakage during operation is due to pre-damaged cells during soldering. Bouraiou *et al*. [184] reported the existence of microcracks and other detectable failures of mono-c-Si and multi-c-Si in Saharan medium (URERMS) fields. On the contrary, Chandel *et al*. [185] and Sharma and Chandel [186] performed a field study on mono-c-Si and multi-c-Si PV modules which were exposed under real operating conditions for 28 years in India and did not detect any microcracks. Dolara *et al*. [187] performed experimental analysis on multi-c-Si PV modules to evaluate the influence of snail trails on the PV modules performance under real conditions. The findings indicated that the performance reduction was more likely to be caused by cell cracks rather than snail trails. Many researchers used indoor testing set ups and studied the fracture strength and therefore the formation of cracks, the crack characteristics and their effect on the electrical characteristics of the PV module.

7.1. Investigations on strength

Fractures are responsible for material, energy and hence, economical losses during the manufacturing process. Therefore, besides the electrical properties, it is equally important to investigate the mechanical and thermophysical properties and especially the material strength. PV modules on the market today offer a 25-year warranty and their reliability and durability over this time period is considered as proven. In practice though, there is currently no available parameter describing the mechanical strength of cells and wafers, which secures the reliability of a specific module. While various module designs have been developed to address the aforementioned challenges, there is no single design that has addressed all the challenges.

7.1.1. Theoretical background

Fracture strength is limited by the structural defects, which may act as stress concentrators [188], [189]. For silicon wafers, microcracks are the most common stress-raisers and the silicon fracture strength is dominated by the number and size of microcracks [3]. Fracture is initiated at these cracks if the stresses become high enough [43]. The fracture strength represents the ability of a given material to resist to crack propagation and it is defined as the limit of energy before two single atoms are separated. Due to the

anisotropy of mono-c-Si, the value of fracture strength for Si wafers along different material directions varies. The actual value of material strength is lower than the theoretical values because of the various defects [111], [190].

There are various test methods for characterising the strength of brittle materials like silicon wafers. In the PV industry the twist test and other test methods like uniaxial and biaxial bending tests are often used and discussed [189], [191]–[193]. Uniaxial bending tests like the three-point bending (3PB) and four-point bending (4PB) are the most common setups that determine the fracture strength of a material (Figure 10). These tests impose high tensile stresses at the centre of the lower edges where a crack initiates and propagates. The distribution of stresses along the specimen can be calculated analytically for a monolithic beam or plate. Biaxial bending test like ring-on-ring and ball-on-ring test lead to a biaxial stress field at the specimen centre at the tensile region, hence, edge defects are excluded [194]. Due to the large deflections there is no analytical solution to calculate the stress from the measured force and therefore FEA calculations need to be implemented to get the correct fracture stress.

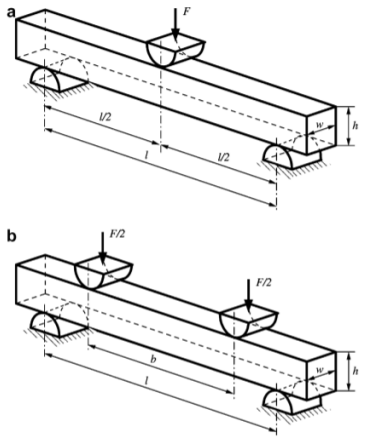

Figure 10. Schematic drawing of (a) a 3-point-bending and (b) 4-point bending test [190]. The test specimen is supported by two rolls at the bottom side and is loaded by one roll (3-point bending) or by two rolls (4-point bending) on the top side.

Due to the brittle nature of silicon, the strength data scatter and it is difficult to find a single value of fracture strength. Therefore, a statistical approach using Weibull analysis is commonly adopted in many studies to determine the fracture strength of wafers [195]–[197]. The characteristic strength σ_θ and the Weibull modulus m are the two parameters which are determined by a Weibull evaluation. The probability of failure P_f represents the probability that a specimen breaks at a specific stress σ.

$$P_f(\sigma) = 1 - e^{-\left(\frac{\sigma}{\sigma\theta}\right)^m} \quad (4)$$

where σ_θ is the characteristic strength which describes the stress for a probability of failure equal to 63.2% and m is the Weibull modulus which describes the scattering of the fracture stresses (small values of m reveal large scatter in strength).

7.1.2. Experimental investigation on the wafer level

A residual microcrack in the wafer after sawing is the main source of breakage in PV silicon substrates [43]. A microcrack behaves like a stress concentrator, which may cause an unstable propagation, even at small loads, particularly during handling and processing of thin Si wafers. The fracture strength of multi-c-Si wafers depends upon both material properties such as grain size, and orientation and defects such as microcracks [198]. Edge microcracks are the most crucial roots of degradation of mechanical strength. Reducing the initiation of microcracks in Si cells will increase the fracture strength [199]. Funke *et al*. [44] implemented biaxial tests to study the behaviour of different wafer types and finite element analysis to calculate the fracture stress. It was shown that the distribution of fracture strength depends on the surface preparation of the wafers. The typical crack depth in wafer for multi-wire slurry sawing process is 10-20 μm [33]. After removing 10 μm of each surface by etching, the fracture stress increases and after the etching of 20 μm of specimen surface, the fracture stress increases even more. Coletti *et al*. [200] used a ring-on-ring bending tester to determine the influence of saw damages as well as etching treatments on the mechanical strength independently of edge damages. It was concluded that the saw damage significantly affects the mechanical integrity of as-cut wafers and that the critical fracture stress can be 60% less compared to etched wafers. Another experimental study with 4-point bending test, showed that polishing or etching of the silicon wafer can increase the strength by 33% compared to as-cut wafers [201]. Schneider *et al*. [202] performed twist tests on multi crystalline silicon cells to investigate the influence of wafer thickness on fracture force. The results showed a strong decrease of stability for thinner wafer materials. Alkaline etching and the application of isotropic texturing increased stability in the range of 10-50% for different thicknesses. Popovich [199] investigated the effect of processing parameters and reported that the strength of the multi-crystalline silicon wafer was increased by approximately 50% after saw damage etching. A linear relationship between fracture load and wafer thickness was reported by Coletti *et al.* [123]. These findings suggest that microcracks will be more crucial as the wafer thickness decreases. Klute *et al*. [203] studied the fracture initiation for as-cut mono-c-Si wafers using fractography. The initial crack was positioned in {100} direction and the direction changes at the start of breakage in the {110} crack propagation direction. The results showed that all silicon wafers with high and low fracture stresses follow the same breakage mechanism indicating the same root cause of failure. Popovich *et al*. [204], [205] underlined the impact of the crystallinity on wafer strength with 4PB tests. Higher strength was found in specimens with a large grain in the centre compared to those with many small grains. In order to exclude the effect of edge defects that appear in 4-point bending tests, biaxial test (ring-on-ring) was performed by Popovich *et al.* [206]. It was found that silicon crystallinity and the position where the wafer is extracted from the cast Si ingot can significantly affect the strength. In other words, wafers taken from the top of the ingot are 30% weaker than those who were taken from the top. Gustafsson *et al*. [96] performed twist tests to investigate the relation between mechanical strength and cracks. They observed that breakage force is dependent on crack geometry and position. Microcracks positioned at the edge of the Si wafer causes breakage at lower forces compared to the microcracks located in the interior.

7.1.3. Experimental investigations on silicon solar cells

The fracture toughness within a mono-c-Si cell with Vickers micro-hardness indentation was investigated in [108]. The mechanical strength of mono-c-Si solar cells with different loading configurations relative to busbars was studied by Kaule *et al.* [207]. The authors implemented 4-point bending tests to 200 mono-c-Si solar cells and the analysis showed that the cell strength depends on the loading direction. Popovich *et al*. [208] carried out 4PB tests on Si solar cells and reported that higher

drying and lower firing temperatures decrease the cell strength in tensile stress. Kohn *et al*. [80], [209] performed ring-on-ring tests and showed that the firing process for various paste materials (AgAl and Al) can decrease the cell strength. It was also noted that during the fracture tests, cracks in the AgAl/Al overlap area act like stress raisers and may lead to fracture at lower stress.

7.2. Investigations of crack characteristics

The crack formation due to the application of homogenous SML was analysed by Kajari-Schröder *et al.* [99]. In this study, the criticality of crack directions was investigated by examining the maximum cell region that may become separated by a single crack of a certain direction. It was observed that different crack directions can have a different impact on the PV power output.

The crack pattern in encapsulated Si solar cells based on 4PB tests was investigated by Sander *et al.* [210]. The results indicated that loading parallel to the busbars is more crucial than perpendicular especially for multi-c-Si cells. The load-displacement curve obtained from this test is shown in Figure 11 where the brittle fracture as soon as the crack propagates is shown. The influence of the mounting configuration on the static and dynamic performance of the PV modules was also investigated with a numerical simulation by Dong *et al.* [174].

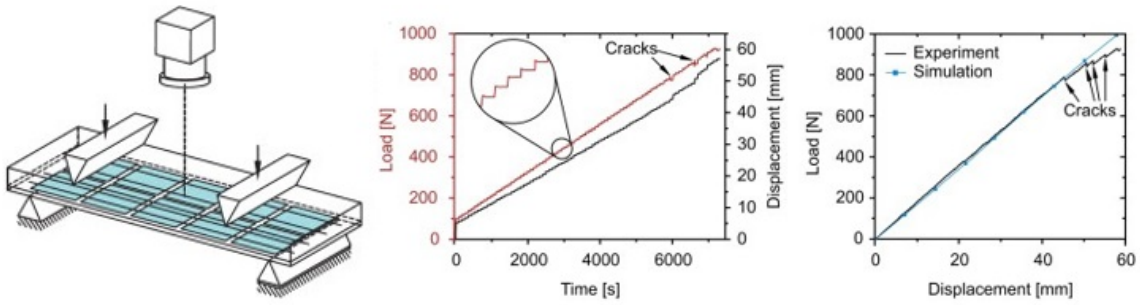

Figure 11. 4PB test setup for the experimental analysis of the impact of mechanical loading on mini modules (left); Load and displacement curves over time of a test specimen (centre); Measured and simulated load over displacement curve (right) [210].

Gabor *et al*. [140] performed an experimental study on a multi-c-Si module. The module tested with Loadspot under steadily increasing and decreasing loads while taking EL images in all stages. They have reported that no cracks were observed in the beginning of the tests, but new cracks were created at 1200 Pa. Upon removing the pressure, the cracks completely closed and became invisible.

Although PV modules are working in a dynamic environment, the general certifications of PV include only static tests [20], [211]. Some researchers have performed experiments and simulations in order to study the effect of the dynamic loading on PV modules. Mülhöfer *et al*. [212] performed cyclic and static ML tests at 25, -20, -40 °C. The results showed a correlation between occurrence of cell cracks and the temperature at which the ML was applied. Schneller *et al*. [166] studied the response cracks to the high number of opening and closing cycles. It was observed that modules that had additional support in the form of back rails, performed better compared to those without such support. It was also observed that damage was more severe in mono crystalline modules at similar load levels. Borri *et al*. [213] have performed cyclic axial deformation and cyclic bending tests on flexible multi-c-Si PV mini-modules and quantified crack propagation.

The effect of the mechanical stress on the appearance of microcracks in PV modules under emulated dynamic conditions was presented by Novickij *et al*. [214] where two resonance frequencies of vibrations (9.8 Hz and 17.5 Hz) caused the appearance of microcracks. The cracks were qualitatively analysed using the electroluminescence technique. The authors concluded that low frequency mechanical loads simulating windy conditions may cause significant damage to the Si cell and hence reduce the performance of the PV module.

7.3. Impact of cracking on electrical characteristics

Static, dynamic and accelerated ageing tests have been performed by many researchers in order to study the effect of cell cracks on the electrical characteristics of the PV modules. A solar cell generated current is proportional to the cell active area. The inactive area can be categorised by whether the current collection from the finger to the busbar is blocked or not. It is observed that if the microcracks cause disconnected cell areas they degrade the electrical performance as well as the mechanical integrity of these cells. Grunow *et al*. [57] reported that when cracks were parallel and centred between the busbars, a power loss of up to 4% occurred. Nevertheless, if the cracks were parallel on both sides of both busbars a power loss of 60% occurred. Therefore, it becomes necessary to understand the influence of microcracks on the electrical characteristics and be able to quantify the risk of power loss in PV modules with cracked cells to ensure their output during the service life.

Paggi *et al*. [101] performed bending tests on flexible mini modules with initial cracks in order to analyse the crack propagation and degradation of the solar cells. The role of fracture on the electrical degradation was monitored during the experiment using the electroluminescence technique. This experimental study showed that crack propagation is a complex phenomenon and cracked areas can recover since the electrical behaviour of cracks depends on the elastic deformation. Gade *et al*. [100] performed experiments to predict the power loss from cell cracks during the lifetime of the module. The authors performed 3-point bending and humidity freeze (HF) tests on mini modules and they have proved that under stressed conditions, cell areas become isolated. Moreover, they have found that the electrical conductivity is restored when the stress is released and that the type of backsheet also influences it. The influence of static and dynamic load tests and their interplay with climatic stress tests were compared by Koch *et al.* [215]. Various test combinations were rated based on the power degradation and on possible changes that have been detected via electroluminescence. It was found that SML tests increase the microcracks and cracked cells due to the higher pressure as set out in the standards for the SML test. Power degradation is higher in the range of 2% for the SML test. Chang *et al*. [216] performed dynamic mechanical load tests (DML) to emulate cell cracking from the wind load during typhoon, and another test sequence with different wind pressure and module framing is utilised to evaluate subsequent degradation in the field. The authors used three types of module framing structures which showed different power degradation after the test sequence and proved that the mounting configuration plays a significant role for a PV system's quality in the field.

A major cause of potential induced degradation (PID) for p-type Si solar cells is sodium (Na) ion migration from the glass through the encapsulant into the Si cell. There have been some experimental investigations on microcrack related PID problem and its mechanism. The effect of microcracks in silicon solar cells on the PID behaviour was investigated by Gou *et al.* [27]. The local current density-voltage (JV) characteristics and EL images of the mini modules with existing microcracks of different lengths were characterised before and after the PID test. The results indicated that as the microcrack length increases, the PV modules tend to show a more serious PID behaviour. Another experimental work proved that the microcrack related shunt area is influenced by the length the width and depth of cell microcracks [217].

They have investigated the impact and mechanism of microcracks exposed on Na ion on the evolution of PID. The IV curve attributes in the microcracked areas of the Si solar cells which were measured before and after PID stress tests proved the presence of microcrack related PID shunts. Electroluminescence and LIT were used to detect PID shunts related to microcracks in every stage of the experiment as it is shown in Figure 12.

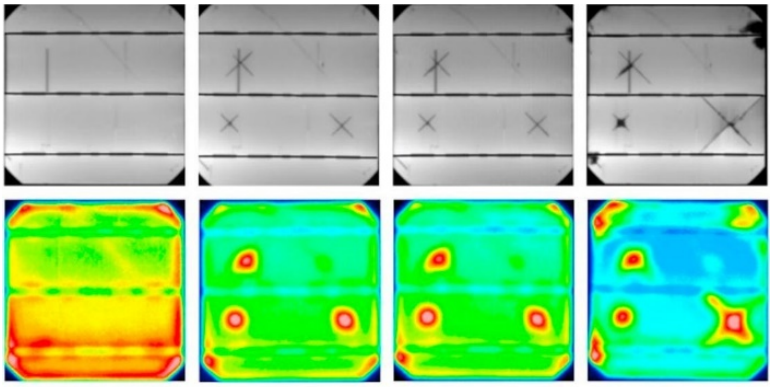

Figure 12. Electroluminescence (top row) and Lock-in thermography (bottom row) images of PID shunts related to microcracks (a) initial condition , (b) after forming the microcracks, (c) after 50 hours of PID stress test (d) after 100 hours of PID stress test [217].

Research has shown that cracks may contribute to reverse biasing [218], [219] which can cause a temperature increase and therefore, raise degradation issues. Käsewieter [220] performed a bending test on laminates and found that the silver front side metallization cracked simultaneously with the Si material. When the mechanical load was removed, the front side metallization reconnected almost without any additional contact resistance. On the contrary, the aluminium rear side metallization was not instantly isolated with the first cracking of the silicon but exhibited a fatigue cracking behaviour. As the width and depth of microcracks increases, the higher the crack resistance becomes [220]. The high resistances hinder the carrier transportations to the fingers, reduce the carrier collection probability and a rapid recombination of carriers at the edges of the microcracks is observed. Therefore, these areas become recombination centres, which leads to strong degradation in the corresponding External Quantum Efficiency (*EQE*) responses [217]. As a result, the larger the width and depth of the microcrack is, the higher the degradation of *EQE* and other electrical attributes will be. Demant *et al*. [221] investigated the influence of cracks induced in early processing steps on the shunting behavior of Si cells. The findings revealed that the microcracks led to a significant power degradation due to increased reverse current density j_{REV} and a reduced parallel resistance R_p which was observed through photoluminescence (PL) imaging.

7.3.1. Effect of accelerated ageing tests on the electrical characteristics

Typically, PV manufacturers offer a product guarantee of 15 years and 10- and 25-year PV performance warranties of 90% and 80% of the rated power respectively. As part of the certification process, PV modules are subjected to mechanical load (static and dynamic) and several types of accelerated aging tests as thermal cycling, damp heat and humidity freeze, which are described in the international standard IEC 61215 [20]. The purpose of these tests is to verify the durability and reliability of the products; i.e. the ability of the modules to withstand thermal mismatch, fatigue and other stresses caused by repeated changes on

767 temperature and humidity [20]. Among these tests is the Thermal Cycling Test (TCT) where a module is
768 subjected to relative humidity of 85% and temperature cycles between -40°C and +85°C as depicted in
769 Figure 13.

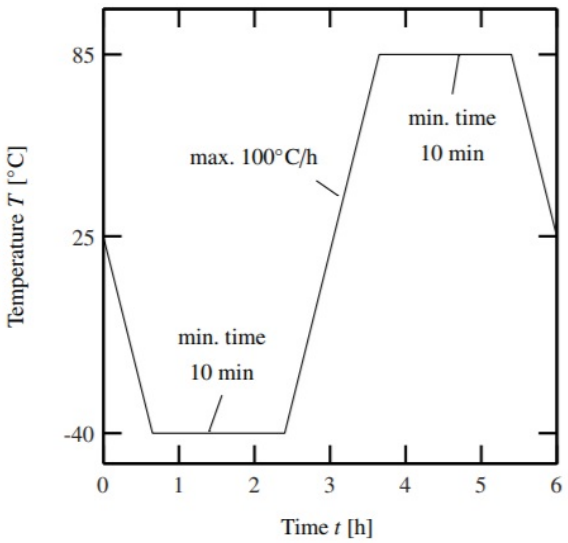

770

771 **Figure 13.** One cycle of the thermal cycling test (TCT) according to IEC 61215 [20].

772 Many PV modules degrade more than 5% after the accelerated aging tests and therefore they fail [158].
773 The evolution of microcracks due to thermal cycles is still not clear [223]. The impact of accelerated aging
774 test on the formation of microcracks in PV module was investigated by González *et al.* [224] where it was
775 reported that the thermal cycles applied to the PV modules which were uninstalled from a PV plant
776 produced no new microcracks but predisposed the PV modules to cracking in subsequent mechanical
777 testing. After the TCT and ML, the power loss was between 0.4-1.8%. While in another experiment [15] it
778 was reported that the P_{MPP} and *FF* were decreased by 3.6% and 3% after the mechanical load test and 6%
779 and 6.2% after mechanical load testing and 200 thermal cycles (i.e. TC200) combined. Another study
780 reported no significant power losses after observing a crack growth; even after 800 TC cycles, the modules
781 retained more than 95.5% of the initial power [222]. Kontges *et al*. [8] performed a ML test which was
782 followed by 200 HF cycles and correlated the power loss with the number of cracks in a PV module (see
783 Figure 14). They observed that mode A cracks cause low power loss (as low as 4.3%) but during the
784 humidity freeze test they can become mode B or C cracks and therefore can cause a significant power loss
785 (of up to 9.6%).

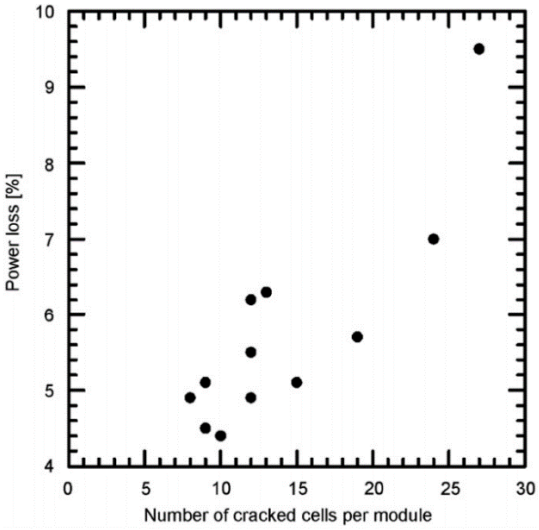

Figure 14. Diagram which shows the correlation between the power loss after a ML test succeeded by 200 HF cycles with the number of cells which cracked during the ML test. Each point represents a single PV module [8].

The long-term reliability of PV modules and the power loss using accelerated aging tests was also studied by Khatri *et al.* [14]. Damp heat (DH) test mainly degrades the module components that allows moisture and heat to react with the solar cells and cause degradation. The experimental results by Khatri *et al*. [14] revealed an increase in the series resistance of the cell of about 7% due to cracking with a power loss of 4% and a fill factor reduction of 3%. Microcracks, observed mainly during TCT, could be critical for the long-term reliability of PV modules and thus should be suppressed as much as possible. A significant increase in cracks was observed in previously undamaged modules when more than 300 thermal cycles were applied. Similar results were obtained by Philipp [225] who reported that 50% of the modules tested exhibited 3 or less new cracks after TC200. However, in the same report, the author also showed that even after TC400, 10% of the modules did not show any additional cracks. Less than 5% of the tested modules will degrade more than 5% after TC200 and TC400. Lincoln *et al*. [226] performed an experimental analysis with stress testing which included static mechanical load, environmental chamber testing and cyclic loading accompanied with EL and IV. It was concluded that thermal cycling and humidity freeze sequences make the PV modules more vulnerable. It was also reported that previously created cracks can be reopened at lower load levels, a result which was also observed by Sander *et al.* [210]. An investigation of more than 250 PV modules found power losses of up to 20% caused by cell cracks in combination with ethylene-vinyl acetate (EVA) browning and delamination [13]. Kajari-Schröder *et al.* [16], found that after 200 HF cycles, 7% of the cracked cells developed an electrically inactive cell area and 29% of the cracked cells exhibited power degradation which was not quantified.

In addition to the previous works, accelerated ageing tests were performed to pre-damaged modules and their degradation was analysed. Grunow *et al*. [227] induced cracks to mono-c-Si cell PV modules, to study the effect of the location of the cracks on the electrical parameters of individual Si cells**.** Wendt *et al*. [228] investigated a PV module whose solar cells were soldered under inappropriate conditions so that cracks were induced. The module was stressed by TC250 and HF10. In these tests, damages including crack growth were observed already after the first 50 thermal cycles, which is in contrast to the observations of the study of Camus *et al*. [229]. There, pre-damaged modules were exposed to various accelerated aging

conditions in order to analyse the impact of the pre-existing damage on the degradation behaviour under the respective aging scenario. The authors observed that none of the accelerated aging tests caused any change in the pre-existing damage and that the behaviour and rate was dependent on the choice of the module components rather than the nature of the pre-damage. Table 6 presents a summary of the experimental investigations related to cracks in c-Si PV.

821 **Table 6.** Summary of experimental investigations related to PV cracks.

Reference	Indoor/ outdoor	Static/ Dynamic	ML Setup	Sequence of test	Scale	mono or multi	Detection method of cracks	Electrical characteristics measured	Results and remarks
Kajari-Shroder *et al*. [99]	I	S	In house static mechanical load tester (5x3 suction cups)	-	Modules-60 cells	mono and multi	EL	-	1) Each crack orientation can influence power output of PV modules in a different way, 2) a homogenous pressure leads to inhomogeneous distribution of cracks due to the frame supporting of the PV module, 3) the spatial distribution of the different crack classes differs strongly.
Kontges [8]	I	S	In house static mechanical load	ML-HF200	Modules-60 cells	multi	EL	✓	Cell microcracks cause a low power loss when they do not cause disconnected regions areas (mode A). During HF some mode A cracks change to mode B or even mode C. Power loss is higher for modules with a higher number of cracked cells.
Sander *et al*. [210]	I	S	4PB	ML	Mini modules-10 cells	mono and multi	EL	-	1) Loading parallel to busbars is more critical than perpendicular especially for multi-c-Si, 2) the cracks initiate preferentially at existing weak-spots from the soldering or lamination process.
Gabor *et al*. [140]	I	S	Loadspot	-	Module	multi	EL	✓	Initially no cracks were observed but many new cracks formed at 1200 Pa. Upon releasing all pressure, the cracks fully closed and were undetectable. The modules with open crack cells can incur more power loss upon shading that the modules without open crack cells.
Paggi *et al*. [101]	I	D	PMMA balls to create pre-existing cracks & bending test	-	Semi-flexible mini module-10 cells	mono	EL	✓	Electrical behaviour of cracks depends on the elastic deformation. Cracked regions can recover the electric conductivity.
Gade *et al*. [100]	I	S	3PB	3PB & HF10 and some modules + HF20	Mini modules-4 cells	multi	EL	✓	Under stressed conditions, the cracked areas of the cell lose electrical conductivity with the rest of the cell circuit. Electrical conductivity is restored when the stress is removed. The type of backsheet influences the electrical conductivity.
Koch *et al*. [215]	I	S, D	16 pneumatic cylinders, each of them equipped with four vacuum cups	ML-DH, DML-DH, DH	Module-72 cells	mono	EL	✓	Power degradation is in the range of 2% for the ML which is higher than DML. DH results in a power increase of +2% in average on mono-c-Si modules which is in agreement with the IEC certification test procedure with an average increase of 1%.
Chang *et al*. [216]	I, O	D	Vacuum cups	DML, DML-TC50-HF10	Module	mono and multi	EL	✓	Outdoor measurements after two sequential typhoons (with the maximum wind speed: 35.7 m/sec and 36.2 m/sec) show a power degradation of 1.5% and 1.6% for mono-c-Si and multi-c-Si PV module respectively.
Mülhöfer *et al*. [212]	I	S, D	Pneumatic cylinders and sandbags	ML, DML	Module	mono and multi	EL	✓	Cyclic loading result in less power loss and cell defects compared to the quasi static load. More power loss was observed for mono-c-Si modules. Mechanical load test at -40 °C resulted in many cell cracks and a significant loss of power. Testing at -40 °C with sandbags instead of pneumatic cylinders shows also significant cell damages.

									The tests have unveiled a correlation between occurrence of cell cracks and the temperature at which the mechanical load was applied.
Schneller *et al*. [166]	I	D	Loadspot	ML-DML	Module-60 cells	mono and multi	EL	✓	Modules with additional support such as backrails perform better compared to those who have no support. Although both mono-c-Si and multi-c-Si modules had a similar number of fractured cells, the mono-c-Si module had a power loss up to 20% whereas the multi-crystalline module only had 5.3%.
Hacke *et al*. [222]	I	-	-	DH, TC, alternating DH & TC	Module	multi	Optical inspection, thermography, EL	✓	1) A small number of crack growth was observed after TC200 with an ineligible power loss, 2) the modules retained more than 95.5% of the initial power after TC800.
Dethlefsen *et al*. [223]	I	-	-	TC	Module	multi	EL	✓	Even modules with a relatively large number of cracked cells do not impact the degradation even after a prolonged IEC 61215 testing time.
Chatuverdi *et al*. [15]	I	S	ML (uniform-2400 Pa)	ML, ML-TC	Module-60 cells	multi	EL,SEM	✓	P_{MPP} and FF of the module after mechanical load test decreased by 3.6% and 3.0% respectively, while the V_{OC} and the I_{SC} largely remain unaffected in this experiment. This can be interpreted as changes to the shunt and series resistance.
Gonzalez *et al*. [224]	I,O	S	ML 2400 Pa (IEC 61215)	TC-ML, ML	Module	multi	EL	✓	The thermal cycles applied to the PV modules did not produce any new microcracks but predisposed the PV modules to cracking in subsequent mechanical testing while during the TC-ML, the cracks mostly occurred parallel and 45 degrees the busbars. Existing microcracks have not grown visibly after either the ML or TC-ML and therefore the presence of microcracks did not imply a higher microcrack formation in the future. The power loss was between 0.4-1.8% after TC and ML.
Khatri *et al*. [14]	I	-	-	TC, DH	Module-60cells	multi	EL	✓	Loss in FF (due to an increase in R_S) was observed during both the accelerated tests and was one of the main causes of module degradation. DH mainly degrades module's components which allow moisture and heat to react with cells and degrade them.
Lincoln *et al*. [226]	I	S,D	Loadspot	ML-PCO test-TC-HF	Modules-60 cells	mono	EL	✓	TC/HF sequence made PV modules more vulnerable to future loads. Existing cracks can be re-opened at lower load levels that was used to form these cracks.
Kajari-Shroder *et al*. [16]	I	S	In house static mechanical load tester	ML-HF	Modules-60 cells	mono and multi	EL	✓	Cracks parallel to busbars and cells with several cracking directions exhibited a high probability of degradation in artificial aging.
Sander *et al*. [52]	I,O	S	4PB	DH-ML, TC-ML	Mini modules-6 cells	mono	EL	-	1) The investigation of varied manufacturing conditions showed that infrared soldering was superior. 2) After DH-ML: the fracture strength has increased. 3) After TC-ML: the fracture strength has significantly reduced already after the first 10 cycles. 4) After 4-month outdoor exposure no significant change in the characteristic strength could be measured.

8. Summary and Conclusions

Cracks in wafer-based silicon solar cells are a well-known problem in the PV industry. Their formation is inevitable during either the manufacturing or the service life of a module and up to now it is not clear how to quantify their impact on PV performance. Undetected microcracks that were formed during production, can result in a reduction of the expected service lifetime. Areas of Si cells can be partially or fully isolated by cracks and their impact on power loss depends on their characteristics. Cracks potentially evolve over prolonged periods of time and thus extend their effect on the functionality and performance of a PV module, potentially triggering hot spots as well. Some recent studies have shown that microcracks can enhance the phenomenon of PID. Thermographic studies show that cracks are acting primarily as recombination centres with a local increase in temperature around them and therefore the efficiency of the PV module may be reduced. In the literature, cracks in PV modules have been strongly investigated, since due to mechanical or thermal loads they can significantly reduce the electrical performance and reliability of modules.

This study summarised and compared various aspects of cracks in PV modules such as their origin, their characteristics and factors that affect them. Cracks may be formed during the cutting process of an ingot or crystal bar or during the different production stages. Moreover, improper PV module handling/transportation/installation and external environmental loads in the field can lead to formation of new cracks or propagation of the existing ones. In this study cracks were classified based on their size, shape, position, direction or their severity and the factors affecting them were loosely considered as two-fold: (i) those deriving from mechanical properties and (ii) those resulting from their geometrical properties.

Numerical simulations that were performed for studying the residual stresses in PV production and operation, which can lead to initiation or propagation of cracks were examined in detail. Furthermore, other studies that used methods from fracture mechanics trying to correlate cracks with their electric response were also discussed. In addition, experimental studies that have been implemented in the wafer-, cell- and PV-module scale to investigate the effect of cracks on structural strength and the electrical characteristics of the module have been compared according to the application, detection methods and materials used. In order to improve the functionality and performance of the PV modules, understanding the fracture mechanism in silicon is of great significance for both industrial and scientific practitioners.

The main finding of this comprehensive literature review showed that the crack characteristics (location, orientation, shape etc.) depend strongly on how they were initiated. Furthermore, the review of crack simulation studies showed that most of them have not incorporated the residual stresses from the previous production and handling steps, neglecting the stress history of the Si cells. As such, an underestimation of cracking probability arises especially when the PV modules operate in the field where they experience varying loading conditions due to different environmental parameters. This study also showed that the effect of cracks on the reliability and electrical characteristics of PV modules is debatable. While several studies have shown that an electric recovery can be achieved when the applied load is withdrawn, others reported a power loss of up to 20% (combined with other degradation mechanisms). Although cracks are unavoidable, identifying and understanding the factors that trigger crack initiation and propagation is crucial for the improvement of the mechanical and electrical reliability of the PV modules. Therefore, further investigations need to be conducted in order to a) realise whether or not PV modules that are exposed under different loading conditions, with or without pre-operation caused stresses, exhibit performance losses or degradation issues, and b) to predict and quantify the long-term impact and evolution of cracking under different meteorological conditions.

Acknowledgement

This work has been co-financed by the European Union's Horizon 2020 research and innovation programme in the framework of "TwinPV" project with the grant agreement number 692031.

References

[1] "International Technology Roadmap for Photovoltaic (ITRPV) Ninth Edition. Results 2017," 2018. [Online]. Available: http://www.itrpv.net/Reports/Downloads/2018.

[2] M. Knausz *et al.*, "Thermal expansion behavior of solar cell encapsulation materials," *Polym. Test.*, vol. 44, pp. 160–167, 2015.

[3] P. Rupnowski and B. Sopori, "Strength of silicon wafers: fracture mechanics approach," *Int. J. Fract.*, vol. 155, no. 1, pp. 67–74, 2009.

[4] S. Pingel, Y. Zemen, O. Frank, T. Geipel, and J. Berghold, "Mechanical stability of solar cells within solar panels," *in 24th European PV Solar Energy Conference*. Hamburg, Germany, pp. 3459–3464, 2009.

[5] A. M. Gabor, R. Janoch, A. Anselmo, and H. Field, "Solar panel design factors to reduce the impact of cracked cells and the tendency for crack propagation," *in NREL PV Module Reliability Workshop*. Denver, CO, USA, pp. 1–11, 2015.

[6] M. Köntges, M. Siebert, A. Morlier, R. Illing, N. Bessing, and F. Wegert, "Impact of transportation on silicon wafer-based photovoltaic modules," *Prog. Photovoltaics Res. Appl.*, vol. 24, no. 8, pp. 1085–1095, 2016.

[7] M. Assmus, S. Jack, K. Weiss, and M. Koehl, "Measurement and simulation of vibrations of PV-modules induced by dynamic mechanical loads," *Prog. Photovoltaics Res. Appl.*, vol. 19, no. 6, pp. 688–694, 2011.

[8] M. Köntges, I. Kunze, S. Kajari-Schröder, X. Breitenmoser, and B. Bjørneklett, "The risk of power loss in crystalline silicon based photovoltaic modules due to micro-cracks," *Sol. Energy Mater. Sol. Cells*, vol. 95, no. 4, pp. 1131–1137, 2011.

[9] S. Spataru, P. Cernek, D. Sera, T. Kerekes, and R. Teodorescu, "Characterization of a Crystalline Silicon Photovoltaic System after 15 Years of Operation in Northern Denmark," *in 29th European Photovoltaic Solar Energy Conference and Exhibition*. Amsterdam, Netherlands, pp. 2680–2688, 2014.

[10] M. A. Munoz, M. C. Alonso-García, N. Vela, and F. Chenlo, "Early degradation of silicon PV modules and guaranty conditions," *Sol. Energy*, vol. 85, no. 9, pp. 2264–2274, 2011.

[11] J. I. van Mölken *et al.*, "Impact of Micro-Cracks on the Degradation of Solar Cell Performance Based On Two-Diode Model Parameters," *Energy Procedia*, vol. 27, no. Supplement C, pp. 167–172, 2012.

[12] B. Javvaji, P. R. Budarapu, M. Paggi, X. Zhuang, and T. Rabczuk, "Fracture Properties of Graphene-Coated Silicon for Photovoltaics," *Adv. Theory Simulations*, vol. 1, no. 12, p. 1800097, 2018.

[13] K. Schulze, M. Groh, M. Nieß, C. Vodermayer, G. Wotruba, and G. Becker, "Untersuchung von Alterungseffekten bei monokristallinen PV-Modulen mit mehr als 15 Betriebsjahren durch Elektrolumineszenz- und Leistungsmessungen," *in 28th Symposium Photovoltiasche Solarenergie*. Staffelstein, Germany, 2013.

[14] R. Khatri, S. Agarwal, I. Saha, S. K. Singh, and B. Kumar, "Study on long term reliability of photo-voltaic modules and analysis of power degradation using accelerated aging tests and electroluminescence technique," *Energy Procedia*, vol. 8, no. Supplement C, pp. 396–401, 2011.

[15] P. Chaturvedi, B. Hoex, and T. M. Walsh, "Broken metal fingers in silicon wafer solar cells and PV modules," *Sol. Energy Mater. Sol. Cells*, vol. 108, pp. 78–81, 2013.

[16] S. Kajari-Schröder, I. Kunze, and M. Köntges, "Criticality of Cracks in PV Modules," *Energy Procedia*, vol. 27, pp. 658–663, 2012.

[17] A. Morlier, F. Haase, and M. Köntges, "Impact of Cracks in Multicrystalline Silicon Solar Cells on PV Module Power—A Simulation Study Based on Field Data," *IEEE J. Photovoltaics*, vol. 5, no. 6, pp. 1735–1741, 2015.

[18] M. Köntges *et al.*, *Review of Failures of Photovoltaic Modules. IEA PVPS Task 13*. International Energy Agency (IEA), 2014.

[19] S. Dietrich, M. Sander, M. Pander, and M. Ebert, "Interdependency of mechanical failure rate of encapsulated solar cells and module design parameters," *in SPIE 8472 - Reliability of Photovoltaic Cells, Modules, Components, and Systems V*. San Diego, CA, USA, p. 84720P, 2012.

[20] *IEC 61215. Crystalline silicon terrestrial photovoltaic (PV) modules e design qualification and type approval*. International Electrotechnical Commission (IEC), 2005.

[21] M. Abdelhamid, R. Singh, and M. Omar, "Review of Microcrack Detection Techniques for Silicon Solar Cells," *IEEE J. Photovoltaics*, vol. 4, no. 1, pp. 514–524, 2014.

[22] M. Köntges *et al.*, *Assessment of Photovoltaic Module Failures in the Field. Report IEA PVPS Task 13*. International Energy Agency (IEA), 2017.

[23] "Durable Module Materials Consortium (DuraMat)," 2019. .

[24] M. Israil, S. A. Anwar, and M. Z. Abdullah, "Automatic detection of micro-crack in solar wafers and cells: a review," *Trans. Inst. Meas. Control*, vol. 35, no. 5, pp. 606–618, 2013.

[25] M. Israil, "Non-destructive Microcracks Detection Techniques in Silicon Solar Cell," *Phys. Sci. Int. J.*, vol. 4, no. 8, pp. 1073–1087, 2014.

[26] B. Du, R. Yang, Y. He, F. Wang, and S. Huang, "Nondestructive inspection, testing and evaluation for Si-based, thin film and multi-junction solar cells: An overview," *Renew. Sustain. Energy Rev.*, vol. 78, pp. 1117–1151, 2017.

[27] X. Gou, X. Li, S. Wang, H. Zhuang, X. Huang, and L. Jiang, "The Effect of Microcrack Length in Silicon Cells on the Potential Induced Degradation Behavior," *Int. J. Photoenergy*, vol. 2018, pp. 1–6, 2018.

[28] S. Wieghold, A. E. Morishige, L. Meyer, T. Buonassisi, and E. M. Sachs, "Crack detection in crystalline silicon solar cells using dark-field imaging," *Energy Procedia*, vol. 124, pp. 526–531, 2017.

[29] H. Wu, "Wire sawing technology: A state-of-the-art review," *Precis. Eng.*, vol. 43, pp. 1–9, 2016.

[30] H. Wu, S. N. Melkote, and S. Danyluk, "Mechanical Strength of Silicon Wafers Cut by Loose Abrasive Slurry and Fixed Abrasive Diamond Wire Sawing," *Adv. Eng. Mater.*, vol. 14, no. 5, pp. 342–348, May 2012.

[31] T. Liu, P. Ge, W. Bi, and Y. Gao, "Subsurface crack damage in silicon wafers induced by resin bonded diamond wire sawing," *Mater. Sci. Semicond. Process.*, vol. 57, pp. 147–156, 2017.

[32] R. K. Kang, Y. F. Zeng, S. Gao, Z. G. Dong, and D. M. Guo, "Surface Layer Damage of Silicon Wafers Sliced by Wire Saw Process," *Adv. Mater. Res.*, vol. 797, pp. 685–690, Sep. 2013.

[33] A. Grün, A. Lawerenz, R. Porytskyy, and O. Anspach, "Investigation of wafer surfaces with space-resolved breaking strength tests and corresponding analysis of the crack depth," *in 26th European*

Photovoltaic Solar Energy Conference and Exhibition. Hamburg, Germany, pp. 961–965, 2011.

[34] C. Funke, O. Sciurova, O. Kiriyenko, and H. J. Moller, "Surface damage from multi-wire sawing and mechanical properties of silicon wafers," in *20th European Photocoltaic Solar Energy Conference and exhibition*, 2005, pp. 6–10.

[35] S. Würzner, A. Falke, R. Buchwald, and H. J. Möller, "Determination of the impact of the wire velocity on the surface damage of diamond wire sawn silicon wafers," *Energy Procedia*, vol. 77, pp. 881–890, Aug. 2015.

[36] R. Buchwald, K. Fröhlich, S. Würzner, T. Lehmann, K. Sunder, and H. J. Möller, "Analysis of the Sub-surface Damage of mc- and cz-Si Wafers Sawn with Diamond-plated Wire," *Energy Procedia*, vol. 38, pp. 901–909, 2013.

[37] C. Yang, F. Mess, K. Skenes, S. Melkote, and S. Danyluk, "On the residual stress and fracture strength of crystalline silicon wafers," *Appl. Phys. Lett.*, vol. 102, no. 2, p. 021909, Jan. 2013.

[38] N. Watanabe, Y. Kondo, D. Ide, T. Matsuki, H. Takato, and I. Sakata, "Characterization of polycrystalline silicon wafers for solar cells sliced with novel fixed-abrasive wire," *Prog. Photovoltaics Res. Appl.*, vol. 18, no. 7, pp. 485–490, Jul. 2010.

[39] B. Sopori, S. Devayajanam, and P. Basnyat, "Surface characteristics and damage distributions of diamond wire sawn wafers for silicon solar cells," *AIMS Mater. Sci.*, vol. 3, no. 2, pp. 669–685, 2016.

[40] C. Chung and V.-N. Le, "Depth of cut per abrasive in fixed diamond wire sawing," *Int. J. Adv. Manuf. Technol.*, vol. 80, no. 5–8, pp. 1337–1346, Sep. 2015.

[41] M. Ge, H. Zhu, C. Huang, A. Liu, and W. Bi, "Investigation on critical crack-free cutting depth for single crystal silicon slicing with fixed abrasive wire saw based on the scratching machining experiments," *Mater. Sci. Semicond. Process.*, vol. 74, pp. 261–266, Feb. 2018.

[42] H. Kim *et al.*, "Effect of texturing process involving saw-damage etching on crystalline silicon solar cells," *Appl. Surf. Sci.*, vol. 284, pp. 133–137, 2013.

[43] H. J. Möller, C. Funke, M. Rinio, and S. Scholz, "Multicrystalline silicon for solar cells," *Thin Solid Films*, vol. 487, no. 1–2, pp. 179–187, 2005.

[44] C. Funke, E. Kullig, M. Kuna, and H. J. Möller, "Biaxial Fracture Test of Silicon Wafers," *Adv. Eng. Mater.*, vol. 6, no. 7, pp. 594–598, 2004.

[45] M. Oswald, T. Loewenstein, O. Anspach, J. Hirsch, D. Lausch, and S. Schoenfelder, "On the correlation of surface roughness to mechanical strength and reflectivity of silicon wafers," *in 29th European Photovoltaic Solar Energy Conference and Exhibition*. Amsterdam, Netherlands, pp. 764–768, 2014.

[46] V. A. Popovich, M. Janssen, I. J. Bennett, and I. M. Richardson, "Microstructure and Mechanical Properties of a Screen-Printed Silver Front Side Solar Cell Contact," *EPD Congress 2015*. Cham, pp. 265–272, 2015.

[47] V. A. Popovich, M. P. F. H. L. van Maris, M. Janssen, I. J. Bennett, and I. M. Richardson, "Understanding the Properties of Silicon Solar Cells Aluminium Contact Layers and Its Effect on Mechanical Stability," *Mater. Sci. Appl.*, vol. 04, no. 02, pp. 118–127, 2013.

[48] S. Kim, S. Sridharan, C. Khadilkar, and A. Shaikh, "Aluminum pastes (lead-free/low-bow) for thin wafers," *in 31st IEEE Photovoltaic Specialists Conference*. Lake Buena Vista, FL, USA, pp. 1100–

992 1102, 2005.

993 [49] F. Huster, "Aluminum-back surface field: bow investigation and elimination," in *20th European*
994 *Photovoltaic Solar Energy Conference and Exhibition*, 2005, pp. 635–638.

995 [50] C. Anguiano, M. Felix, A. Medel, D. Salazar, and H. Marquez, "Heating capacity analysis of a
996 focused infrared light soldering system," *in 37th Annual Conference of the IEEE Industrial*
997 *Electronics Society*. Melbourne, Australia, pp. 2136–2140, 2011.

998 [51] M. Felix, C. Anguiano, A. Medel, M. Bravo, D. Salazar, and H. Marquez, "Infrared thermography
999 of BGA's heated by Focused Infrared Light Soldering System," *in 7th International Microsystems,*
1000 *Packaging, Assembly and Circuits Technology Conference*. Taipei, Taiwan, pp. 323–325, 2012.

1001 [52] M. Sander *et al.*, "Influence of Manufacturing Processes and Subsequent Weathering on the
1002 Occurrence of Cell Cracks in PV Modules," *in 28th European Photovoltaic Solar Energy*
1003 *Conference and Exhibition*. Paris, France, pp. 3275–3279, 2013.

1004 [53] H. Schulte-Huxel, S. Blankemeyer, R. Bock, A. Merkle, S. Kajari-Schröder, and R. Brendel, "Aging
1005 behaviour of laser welded Al-interconnections in crystalline silicon modules," *Sol. Energy Mater.*
1006 *Sol. Cells*, vol. 106, pp. 22–26, 2012.

1007 [54] H. Schulte-Huxel, S. Blankemeyer, A. Merkle, V. Steckenreiter, S. Kajari-Schröder, and R. Brendel,
1008 "Interconnection of busbar-free back contacted solar cells by laser welding," *Prog. Photovoltaics*
1009 *Res. Appl.*, vol. 23, no. 8, pp. 1057–1065, 2015.

1010 [55] H. Schulte-Huxel, S. Kajari-Schroder, and R. Brendel, "Analysis of Thermal Processes Driving
1011 Laser Welding of Aluminum Deposited on Glass Substrates for Module Interconnection of Silicon
1012 Solar Cells," *IEEE J. Photovoltaics*, vol. 5, no. 6, pp. 1606–1612, 2015.

1013 [56] K. Komiyama, T. Sasaki, and Y. Watanabe, "Effect of tool edge geometry in ultrasonic welding,"
1014 *J. Mater. Process. Technol.*, vol. 229, pp. 714–721, 2016.

1015 [57] X. Chen, Y. Gong, D. Li, and H. Li, "Robust and easy-repairable superhydrophobic surfaces with
1016 multiple length-scale topography constructed by thermal spray route," *Colloids Surfaces A*
1017 *Physicochem. Eng. Asp.*, vol. 492, pp. 19–25, 2016.

1018 [58] D. W. K. Eikelboom, J. H. Bultman, A. Schonecker, M. H. H. Meuwissen, M. A. J. C. van den
1019 Nieuwenhof, and D. L. Meier, "Conductive adhesives for low-stress interconnection of thin back-
1020 contact solar cells," *in 29th IEEE Photovoltaic Specialists Conference*. New Orleans, LA, USA, pp.
1021 403–406, 2002.

1022 [59] T. Geipel, L. C. Rendler, M. Stompe, U. Eitner, and L. Rissing, "Reduction of Thermomechanical
1023 Stress Using Electrically Conductive Adhesives," *Energy Procedia*, vol. 77, pp. 346–355, 2015.

1024 [60] Y. Zemen, T. Prewitz, T. Geipel, S. Pingel, and J. Berghold, "The Impact of Yield Strength of the
1025 Interconnector on the Internal Stress of the Solar Cell within a Module," *in 25th European*
1026 *Photovoltaic Solar Energy Conference and Exhibition*. Valencia, Spain, pp. 4073–4078, 2010.

1027 [61] G. Dou, D. C. Whalley, C. Liu, and Y. C. Chan, "An experimental methodology for the study of
1028 co-planarity variation effects in anisotropic conductive adhesive assemblies," *Solder. Surf. Mt.*
1029 *Technol.*, vol. 22, no. 1, pp. 47–55, 2010.

1030 [62] M. T. Zarmai, N. N. Ekere, C. F. Oduoza, and E. H. Amalu, "A review of interconnection
1031 technologies for improved crystalline silicon solar cell photovoltaic module assembly," *Appl.*
1032 *Energy*, vol. 154, pp. 173–182, 2015.

[63] R. Ebner *et al.*, "Increased Power Output of Crystalline Silicon Solar Modules by Application of New Module Concepts," *29th European Photovoltaic Solar Energy Conference and Exhibition*. Amsterdam, Netherlands, pp. 171–176, 2014.

[64] H. Xiong *et al.*, "Formation and Orientational Distribution of Cracks Induced by Electromagnetic Induction Soldering in Crystalline Silicon Solar Cells," *IEEE J. Photovoltaics*, vol. 7, no. 4, pp. 966–973, 2017.

[65] W.J.R.Song, S.K.Tippabhotla, A.A.O.Tay, and A.S.Budiman, "Effect of interconnect geometry on the evolution of stresses in a solar photovoltaic laminate during and after lamination," *Sol. Energy Mater. Sol. Cells*, vol. 187, pp. 241–248, 2018.

[66] S. Dietrich, M. Pander, M. Sander, S. H. Schulze, and M. Ebert, "Mechanical and thermomechanical assessment of encapsulated solar cells by finite-element-simulation," *in SPIE - Reliability of Photovoltaic Cells, Modules, Components, and Systems III*. San Diego, CA, USA, p. 77730F, 2010.

[67] K. N. Rengarajan *et al.*, "Low Stress Encapsulants? Influence of Encapsulation Materials on Stress and Fracture of Thin Silicon Solar Cells as Revealed by Synchrotron X-ray Submicron Diffraction," *Procedia Eng.*, vol. 139, pp. 76–86, 2016.

[68] F. Reil, J. Althaus, W. Vaaßen, W. Herrmann, and K. Strohkendl, "The Effect of Transportation Impacts and Dynamic Load Tests on the Mechanical and Electrical Behaviour of Crystalline PV Modules," *in 25th European Photovoltaic Solar Energy Conference*. Valencia, Spain, pp. 3989–3992, 2010.

[69] X. F. Brun and S. N. Melkote, "Analysis of stresses and breakage of crystalline silicon wafers during handling and transport," *Sol. Energy Mater. Sol. Cells*, vol. 93, no. 8, pp. 1238–1247, 2009.

[70] K. A. Weiss, M. Assmus, S. Jack, and M. Koehl, "Measurement and simulation of dynamic mechanical loads on PV-modules," *in SPIE - Reliability of Photovoltaic Cells, Modules, Components, and Systems II*. San Diego, CA, USA, p. 741203, 2009.

[71] G. Mathiak, J. Sommer, W. Herrmann, N. Bogdanski, J. Althaus, and F. Reil, "PV Module Damages Caused by Hail Impact and Non-Uniform Snow Load," *in 32nd European Photovoltaic Solar Energy Conference and Exhibition*. Munich, Germany, pp. 1692–1696, 2016.

[72] Y. Lee and A. A. O. Tay, "Stress Analysis of Silicon Wafer-Based Photovoltaic Modules Under IEC 61215 Mechanical Load Test," *Energy Procedia*, vol. 33, pp. 265–271, 2013.

[73] D. Moore, A. Wilson, and R. Ross, "Simulated hail impact testing of photovoltaic solar panels," *24th Combined environments: Technology interrelations*. Fort Worth, TX, USA, 1978.

[74] G. Mathiak *et al.*, "PV Module Damages Caused By Hail Impact - Field Experience And Lab Tests," *31st European Photovoltaic Solar Energy Conference and Exhibition*. Hamburg, Germany, pp. 1915 – 1919, 2015.

[75] M. Corrado, A. Infuso, and M. Paggi, "Simulated hail impacts on flexible photovoltaic laminates: testing and modelling," *Meccanica*, vol. 52, no. 6, pp. 1425–1439, 2017.

[76] C. Ferrara and D. Philipp, "Why Do PV Modules Fail?," *Energy Procedia*, vol. 15, pp. 379–387, 2012.

[77] C. Buerhop-Lutz *et al.*, "Performance Analysis of Pre-Cracked PV-Modules at Realistic Loading Conditions," in *33rd European Photovoltaic Solar Energy Conference and Exhibition*, 2017, pp. 1451–1456.

[78] J. A. Tsanakas, L. Ha, and C. Buerhop, "Faults and infrared thermographic diagnosis in operating c-Si photovoltaic modules: A review of research and future challenges," *Renew. Sustain. Energy Rev.*, vol. 62, pp. 695–709, 2016.

[79] A. Holt *et al.*, "Surface structure of mono-crystalline silicon wafers produced by diamond wire sawing and by standard slurry sawing before and after etching in alkaline solutions," in *35th IEEE Photovoltaic Specialists Conference*, 2010, pp. 003501–003504.

[80] C. Kohn, M. Hug, R. Kübler, M. Krappitz, and G. Kleer, "Increase of the strength of screen printed silicon solar cells by post treatments," *in 25th European Photovoltaic Solar Energy Conference and Exhibition / 5th World Conference on Photovoltaic Energy Conversion*, no. September. Valencia, Spain, pp. 2062–2065, 2010.

[81] T. Wagner, M. Schuetz, and M. Ammon, "A New Method for Reliable Crack Detection in Wafers and Cells," in *26th European Photovoltaic Solar Energy Conference and Exhibition*, 2011, pp. 2078–2081.

[82] A. M. Gabor *et al.*, "Soldering induced damage to thin Si solar cells and detection of cracked cells in modules," *in 21st European Photovoltaic Solar Energy Conference and Exhibition*. Dresden, Germany, pp. 4–8, 2006.

[83] G. Li *et al.*, "Thermo-mechanical behavior assessment of smart wire connected and busbarPV modules during production, transportation, and subsequent field loading stages," *Energy*, vol. 168, pp. 931–945, Feb. 2019.

[84] S. Nasr Esfahani, S. Asghari, and S. Rashid-Nadimi, "A numerical model for soldering process in silicon solar cells," *Sol. Energy*, vol. 148, pp. 49–56, 2017.

[85] F. Kraemer, J. Seib, E. Peter, and S. Wiese, "Mechanical stress analysis in photovoltaic cells during the string-ribbon interconnection process," *in 15th International Conference on Thermal, Mechanical and Mulit-Physics Simulation and Experiments in Microelectronics and Microsystems*. Ghent, Belgium, pp. 1–7, 2014.

[86] L. C. Rendler *et al.*, "Thermomechanical stress in solar cells: Contact pad modeling and reliability analysis," *Sol. Energy Mater. Sol. Cells*, vol. 196, pp. 167–177, Jul. 2019.

[87] H. Shin, E. Han, N. Park, and D. Kim, "Thermal Residual Stress Analysis of Soldering and Lamination Processes for Fabrication of Crystalline Silicon Photovoltaic Modules," *Energies*, vol. 11, no. 12, p. 3256, Nov. 2018.

[88] Q. Z. Zhang *et al.*, "Numerical investigation on residual stress in photovoltaic laminates after lamination," *J. Mech. Sci. Technol.*, vol. 29, no. 2, pp. 655–662, 2015.

[89] M. Sander *et al.*, "Characterization of PV modules by combining results of mechanical and electrical analysis methods," *in SPIE -Reliability of Photovoltaic Cells, Modules, Components, and Systems III*. San Diego, CA, USA, p. 777308, 2010.

[90] J.-S. Jeong, N. Park, and C. Han, "Field failure mechanism study of solder interconnection for crystalline silicon photovoltaic module," *Microelectron. Reliab.*, vol. 52, no. 9–10, pp. 2326–2330, 2012.

[91] W. J. R. Song, S. K. Tippabhotla, A. A. O. Tay, and A. S. Budiman, "Numerical Simulation of the Evolution of Stress in Solar Cells During the Entire Manufacturing Cycle of a Conventional Silicon Wafer Based Photovoltaic Laminate," *IEEE J. Photovoltaics*, vol. 8, no. 1, pp. 210–217, 2018.

[92] F. Reil *et al.*, "Experimental Testing of PV Modules under Inhomogeneous Snow Loads," in *27th*

European Photovoltaic Solar Energy Conference and Exhibition, 2012, pp. 3414–3417.

[93] R. Pérez and P. Gumbsch, "An ab initio study of the cleavage anisotropy in silicon," *Acta Mater.*, vol. 48, no. 18–19, pp. 4517–4530, 2000.

[94] T.-K. Wen and C.-C. Yin, "Crack detection in photovoltaic cells by interferometric analysis of electronic speckle patterns," *Sol. Energy Mater. Sol. Cells*, vol. 98, pp. 216–223, 2012.

[95] S. A. Anwar and M. Z. Abdullah, "Micro-crack detection of multicrystalline solar cells featuring an improved anisotropic diffusion filter and image segmentation technique," *EURASIP J. Image Video Process.*, vol. 2014, no. 1, p. 15, 2014.

[96] J. Gustafsson, H. Larsson, H. J. Solheim, and T. Boström, "Mechanical Stress Tests on mc-Si Wafers With Microcracks," *in 23rd European Photovoltaic Solar Energy Conference and Exhibition*. Valencia, Spain, pp. 1957–1960, 2008.

[97] F. Kaule, R. Koepge, and S. Schoenfelder, "Damage and Breakage of Silicon Wafers during Impact Loading on the Wafer Edge," *27th European Photovoltaic Solar Energy Conference and Exhibition*. Frankfurt, Germany, pp. 1179–1184, 2012.

[98] M. Trautmann, K. Mangold, M. Hemsendorf, C. Berge, C. Probst, and E. Rüland, "Inline Microcrack Detection and Mechanical Stability of Silicon Wafers," *in 25th European Photovoltaic Solar Energy Conference and Exhibition / 5th World Conference on Photovoltaic Energy Conversion*. Valencia, Spain, pp. 2618–2621, 2010.

[99] S. Kajari-Schröder, I. Kunze, U. Eitner, and M. Köntges, "Spatial and orientational distribution of cracks in crystalline photovoltaic modules generated by mechanical load tests," *Sol. Energy Mater. Sol. Cells*, vol. 95, no. 11, pp. 3054–3059, 2011.

[100] V. Gade, N. Shiradkar, M. Paggi, and J. Opalewski, "Predicting the long term power loss from cell cracks in PV modules," *in 42nd Photovoltaic Specialist Conference*. New Orleans, LA, USA, pp. 1–6, 2015.

[101] M. Paggi, I. Berardone, A. Infuso, and M. Corrado, "Fatigue degradation and electric recovery in Silicon solar cells embedded in photovoltaic modules," *Sci. Rep.*, vol. 4, no. 1, p. 4506, 2015.

[102] T. L. Anderson, *Fracture Mechanics: Fundamentals and Applications, Fourth Edition*. CRC Press, 2005.

[103] K. B. Broberg, "Formulae related to path-independent integrals," in *Cracks and Fracture*, San Diego: Elsevier, 1999, pp. 696–700.

[104] B. Lawn, *Fracture of Brittle Solids*, 2nd ed. Cambridge: Cambridge University Press, 1993.

[105] I.-H. Lin and R. Thomson, "Cleavage, dislocation emission, and shielding for cracks under general loading," *Acta Metall.*, vol. 34, no. 2, pp. 187–206, 1986.

[106] T. Cramer, A. Wanner, and P. Gumbsch, "Energy Dissipation and Path Instabilities in Dynamic Fracture of Silicon Single Crystals," *Phys. Rev. Lett.*, vol. 85, pp. 788–791, 2000.

[107] L. Zhao, D. Bardel, A. Maynadier, and D. Nelias, "Crack initiation behavior in single crystalline silicon," *Scr. Mater.*, vol. 130, pp. 83–86, 2017.

[108] F. Ebrahimi and L. Kalwani, "Fracture anisotropy in silicon single crystal," *Mater. Sci. Eng.*, vol. 268, no. 1–2, pp. 116–126, 1999.

[109] J. A. Hauch, D. Holland, M. P. Marder, and H. L. Swinney, "Dynamic Fracture in Single Crystal

Silicon," *Phys. Rev. Lett.*, vol. 82, no. 19, pp. 3823–3826, 1998.

[110] D. Sherman, "Hackle or textured mirror? Analysis of surface perturbation in single crystal silicon," *J. Mater. Sci.*, vol. 38, no. 4, pp. 783–788, 2003.

[111] M. J. Buehler, H. Tang, A. van Duin, and W. Goddard, "Threshold crack speed in dynamic fracture of silicon," *MRS Proc.*, vol. 978, 2006.

[112] D. Sherman and I. Be'ery, "Shape and energies of a dynamically propagating crack under bending," *J. Mater. Res.*, vol. 18, no. 10, pp. 2379–2386, 2003.

[113] R. F. Cook, "Strength and sharp contact fracture of silicon," *J. Mater. Sci.*, vol. 41, no. 3, pp. 841–872, 2006.

[114] F. Abraham, N.Bernstein, J. Q. Broughton, and D. Hess, "Dynamic Fracture of Silicon: Concurrent Simulation of Quantum Electrons, Classical Atoms, and the Continuum Solid," *MRS Bull.*, vol. 25, 2000.

[115] M. J. Buehler, A. C. T. van Duin, and W. A. Goddard, "Multiparadigm Modeling of Dynamical Crack Propagation in Silicon Using a Reactive Force Field," *Phys. Rev. Lett.*, vol. 96, no. 9, p. 095505, 2006.

[116] T. Fujii and Y. Akiniwa, "Molecular dynamics analysis for fracture behaviour of single crystal silicon thin film with micro notch," *Model. Simul. Mater. Sci. Eng.*, vol. 14, no. 5, pp. 73–83, 2006.

[117] J. Swadener, M. Baskes, and M. Nastasi, "Molecular Dynamics Simulation of Brittle Fracture in Silicon," *Phys. Rev. Lett.*, vol. 89, no. 8, p. 085503, 2002.

[118] M. A. Hopcroft, W. D. Nix, and T. W. Kenny, "What is the Young's Modulus of Silicon?," *J. Microelectromechanical Syst.*, vol. 19, no. 2, pp. 229–238, 2010.

[119] A. Masolin, P.-O. Bouchard, R. Martini, and M. Bernacki, "Thermo-mechanical and fracture properties in single-crystal silicon," *J. Mater. Sci.*, vol. 48, no. 3, pp. 979–988, 2013.

[120] J. J. Hall, "Electronic effects in the elastic constants of n-type silicon," *Phys. Rev.*, vol. 161, no. 3, pp. 756–761, 1967.

[121] M. Paggi, M. Corrado, and J. Reinoso, "Fracture of solar-grade anisotropic polycrystalline Silicon: A combined phase field–cohesive zone model approach," *Comput. Methods Appl. Mech. Eng.*, vol. 330, pp. 123–148, 2018.

[122] C. Bourgeois, E. Steinsland, N. Blanc, and N. F. de Rooij, "Design of resonators for the determination of the temperature coefficients of elastic constants of monocrystalline silicon," *in International Frequency Control Symposium*. Orlando, FL, USA, pp. 791–799, 1997.

[123] G. Coletti, N. J. C. M. van der Borg, S. De Iuliis, C. J. J. Tool, and L. J. Geerligs, "Mechanical strength of silicon wafers depending on wafer thickness and surface treatment," *in 21st European Photovoltaic Solar Energy Conference and Exhibition*, no. September. Dresden, Germany, pp. 2–5, 2006.

[124] M. Brede, "The brittle-to-ductile transition in silicon," *Acta Metall. Mater.*, vol. 41, no. 1, pp. 211–228, 1993.

[125] A. W. Czanderna and F. J. Pern, "Encapsulation of PV modules using ethylene vinyl acetate copolymer as a pottant: A critical review," *Sol. Energy Mater. Sol. Cells*, vol. 43, no. 2, pp. 101–181, 1996.

[126] K. Agroui and G. Collins, "Determination of thermal properties of crosslinked EVA encapsulant material in outdoor exposure by TSC and DSC methods," *Renew. Energy*, vol. 63, no. Supplement C, pp. 741–746, 2014.

[127] G. Oreski and G. M. Wallner, "Damp heat induced physical aging of PV encapsulation materials," *in 12th IEEE Intersociety Conference on Thermal and Thermomechanical Phenomena in Electronic Systems*. Las Vegas, NV, USA, pp. 1–6, 2010.

[128] S. K. Tippabhotla *et al.*, "From cells to laminate: probing and modeling residual stress evolution in thin silicon photovoltaic modules using synchrotron X-ray micro-diffraction experiments and finite element simulations," *Prog. Photovoltaics Res. Appl.*, vol. 25, no. 9, pp. 791–809, 2017.

[129] U. Eitner, M. Pander, and S. Kajari-Schröder, "Thermomechanics of PV modules including the viscoelasticity of EVA," *in 26th European Photovoltaic Solar Energy Conference and Exhibition*. Hamburg, Germany, pp. 3267–3269, 2011.

[130] O. Hasan and A. F. M. Arif, "Performance and life prediction model for photovoltaic modules: Effect of encapsulant constitutive behavior," *Sol. Energy Mater. Sol. Cells*, vol. 122, pp. 75–87, Mar. 2014.

[131] U. Eitner, "Thermomechanics of photovoltaic modules," Martin-Luther-Universität Halle-Wittenberg, 2011.

[132] C. Chen, F. Lin, H. Hu, and F. Yeh, "Residual Stress and Bow Analysis for Silicon Solar Cell Induced by Soldering," *Sol. Cells*, no. May, pp. 1–3, 2008.

[133] C.-M. Lai, K.-M. Lin, and C.-H. Su, "The effects of cracks on the thermal stress induced by soldering in monocrystalline silicon cells," *Proc. Inst. Mech. Eng. Part E J. Process Mech. Eng.*, vol. 228, no. 2, pp. 127–135, 2014.

[134] J. Al Ahmar and S. Wiese, "A crack analysis model for silicon based solar cells," *in 5th International Conference on Thermal, Mechanical and Mulit-Physics Simulation and Experiments in Microelectronics and Microsystems*. Brussels, Belgium, pp. 1–5, 2004.

[135] S. Wiese, F. Kraemer, E. Peter, and J. Seib, "Mechanical problems of novel back contact solar modules," *in 13th International Thermal, Mechanical and Multi-Physics Simulation and Experiments in Microelectronics and Microsystems*. Cascais, Portugal, pp. 1–6, 2012.

[136] W. Gambogi, S. Kurian, B. Hamzavy, J. Trout, O. Fu, and Y. Chao, "The Role of Backsheet in Photovoltaic Module Performance and Durability," *26th European Photovoltaic Solar Energy Conference and Exhibition*. Hamburg, Germany, pp. 3325–3328, 2011.

[137] F. Haase *et al.*, "Impact of Backsheet on Interconnector and Cell Breakage in PV Laminates under Mechanical Loads," *in 29th European Photovoltaic Solar Energy Conference and Exhibition*. Amsterdam, Netherlands, pp. 2477–2483, 2014.

[138] F. Haase, J. Kosewieter, S. R. Nabavi, E. Jansen, R. Rolfes, and M. Kontges, "Fracture Probability, Crack Patterns, and Crack Widths of Multicrystalline Silicon Solar Cells in PV Modules During Mechanical Loading," *IEEE J. Photovoltaics*, pp. 1–15, 2018.

[139] B. Masetty, N. Shiradkar, and S. Patwardhan, "Comprehensive Study of Reliability of Photovoltaic Modules of Various Configuration under Static and Dynamic Mechanical Loading Conditions Using Finite Element Analysis," *in 35th European Photovoltaic Solar Energy Conference and Exhibition*. Brussels, Belgium, pp. 1247–1251, 2018.

[140] A. M. Gabor, R. Janoch, A. Anselmo, J. L. Lincoln, H. Seigneur, and C. Honeker, "Mechanical load

testing of solar panels - Beyond certification testing," *in 44th Photovoltaic Specialist Conference*. Washington, DC, USA, pp. 1–6, 2017.

[141] Y. Zhang *et al.*, "High-Reliability and Long-Durability Double-Glass Module with Crystalline Silicon Solar Cells with Fire-Safety Class A Certification," *in 28th European Photovoltaic Solar Energy Conference and Exhibition*. Paris, France, pp. 3123–3126, 2013.

[142] A. Infuso, M. Corrado, and M. Paggi, "Image analysis of polycrystalline solar cells and modelling of intergranular and transgranular cracking," *J. Eur. Ceram. Soc.*, vol. 34, no. 11, pp. 2713–2722, 2014.

[143] S.-H. Schulze, M. Pander, S. Müller, C. Ehrich, and M. Ebert, "Influence of Vacuum Lamination Process on Laminate Properties – Simulation and Test Results," *in 24th European Photovoltaic Solar Energy Conference*. Hamburg, Germany, pp. 3367–3372, 2009.

[144] R. Mickiewicz *et al.*, "Effect of encapsulation modulus on the response of PV modules to mechanical stress," *in 26th European Photovoltaic Solar Energy Conference and Exhibition*. Hamburg, Germany, pp. 3157–3161, 2011.

[145] M. W Rowell, S. G Daroczi, D. W J Harwood, and A. Gabor, "The Effect of Laminate Construction and Temperature Cycling on the Fracture Strength and Performance of Encapsulated Solar Cells," in *7th World Conference on Photovoltaic Energy Conversion*, 2018.

[146] A. J. Beinert, M. Ebert, U. Eitner, and J. Aktaa, "Influence of Photovoltaic Module Mounting Systems on the Thermo-Mechanical Stresses in Solar Cells by FEM Modelling," in *32nd European Photovoltaic Solar Energy Conference and Exhibition*, 2016, pp. 1833–1836.

[147] J. H. Wohlgemuth, D. W. Cunningham, N. V. Placer, G. J. Kelly, and A. M. Nguyen, "The effect of cell thickness on module reliability," *in 33rd IEEE Photovoltaic Specialists Conference*. San Diego, CA, USA, pp. 1–4, 2008.

[148] B. Terheiden *et al.*, "Manufacturing 100-µm-thick silicon solar cells with efficiencies greater than 20% in a pilot production line," *Phys. status solidi*, vol. 212, no. 1, pp. 13–24, 2015.

[149] P. A. Wang, "Industrial challenges for thin wafer manufacturing," *in 4th World Conference on Photovoltaic Energy Conference*, vol. 1. Waikoloa, HI, USA, pp. 1179–1182, 2007.

[150] Z. Liu, S. Wieghold, L. T. Meyer, L. K. Cavill, T. Buonassisi, and E. M. Sachs, "Design of a Submillimeter Crack-Detection Tool for Si Photovoltaic Wafers Using Vicinal Illumination and Dark-Field Scattering," *IEEE J. Photovoltaics*, vol. 8, no. 6, pp. 1449–1456, 2018.

[151] E. Kurtz, L. Karpowich, D. Moyer, P. Gundel, M. König, and W. Zhang, "Reducing Solar Cell Production Costs Via Low Silver Containing Backside Metallization Pastes," *in 27th European Photovoltaic Solar Energy Conference and Exhibition*. Frankfurt, Germany, pp. 1806–1808, 2012.

[152] H. Chen, C. Chen, M. Chang, C. H. Hsueh, E. Yen, and K. L. Ho, "The Influence of Cell Busbar Pattern on PV Module Reliability," *in 29th European Photovoltaic Solar Energy Conference and Exhibition*. Amsterdam, Netherlands, pp. 2562–2565, 2014.

[153] S. Braun, G. Hahn, R. Nissler, C. Pönisch, and D. Habermann, "The Multi-busbar Design: An Overview," *Energy Procedia*, vol. 43, pp. 86–92, 2013.

[154] J. Burschik *et al.*, "Transition to 4 and 5 BB Designs for Ni/Cu/Ag Plated Cells," *Energy Procedia*, vol. 98, pp. 66–73, 2016.

[155] J. Walter, M. Tranitz, M. Volk, C. Ebert, and U. Eitner, "Multi-wire Interconnection of Busbar-free

Solar Cells," *Energy Procedia*, vol. 55, pp. 380–388, 2014.

[156] S. Braun, G. Micard, and G. Hahn, "Solar Cell Improvement by using a Multi Busbar Design as Front Electrode," *Energy Procedia*, vol. 27, pp. 227–233, 2012.

[157] S. Braun, G. Hahn, R. Nissler, C. Pönisch, and D. Habermann, "Multi-busbar Solar Cells and Modules: High Efficiencies and Low Silver Consumption," *Energy Procedia*, vol. 38, pp. 334–339, 2013.

[158] S. K. Chunduri, "The buzz on busbars: Increasing the number of busbars - and the look of PV - is the latest trend in the CTS world," in *PHOTON International*, 2013, pp. 84–105.

[159] Y. Xie *et al.*, "Performance of Multi-Busbar PV Modules," *in 33rd European Photovoltaic Solar Energy Conference and Exhibition*. Amsterdam, Netherlands, pp. 1639–1642, 2017.

[160] J. Walter, L. C. Rendler, C. Ebert, A. Kraft, and U. Eitner, "Solder joint stability study of wire-based interconnection compared to ribbon interconnection," *Energy Procedia*, vol. 124, pp. 515–525, 2017.

[161] P. Papet *et al.*, "New Cell Metallization Patterns for Heterojunction Solar Cells Interconnected by the Smart Wire Connection Technology," *Energy Procedia*, vol. 67, pp. 203–209, 2015.

[162] G. Schubert, G. Beaucarne, and J. Hoornstra, "The Future of Metallization – Forecast of the Experts of the 5th Metallization Workshop," *Energy Procedia*, vol. 67, pp. 13–19, 2015.

[163] T. Söderström, P. Papet, and J. Ufheil, "Smart Wire Connection Technology," *in 28th European Photovoltaic Solar Energy Conference and Exhibition*. Paris, France, pp. 495–499, 2013.

[164] A. Faes *et al.*, "SmartWire Solar Cell Interconnection Technology," *in 29th European Photovoltaic Solar Energy Conference and Exhibition*. Amsterdam, Netherlands, pp. 2555–2561, 2014.

[165] A. Gabor *et al.*, "Compressive Stress Strategies for Reduction of Cracked Cell Related Degradation Rates in New Solar Panels and Power Recovery in Damaged Solar Panels," *in 7th World Conference on Photovoltaic Energy Conversion*. Waikoloa, HI, USA, 2018.

[166] E. Schneller *et al.*, "Evaluating Solar Cell Fracture as a Function of Module Mechanical Loading Conditions," *in 44th IEEE Photovoltaic Specialist Conference*. Washington, DC, USA, 2017.

[167] H. Nussbaumer, M. Klenk, and N. Keller, "Small Unit Compound Modules: a New Approach for Light Weight PV Modules," *in 32nd European Photovoltaic Solar Energy Conference and Exhibition*. Munich, Germany, pp. 56–60, 2016.

[168] S. Dietrich, M. Pander, M. Sander, and M. Ebert, "Mechanical Investigations on Metallization Layouts of Solar Cells with Respect to Module Reliability," *Energy Procedia*, vol. 38, pp. 488–497, 2013.

[169] S. Wiese, F. Kraemer, N. Betzl, and D. Wald, "Interconnection technologies for photovoltaic modules - analysis of technological and mechanical problems," *in 11th International Thermal, Mechanical & Multi-Physics Simulation, and Experiments in Microelectronics and Microsystems*. Bordeaux, France, pp. 1–6, 2010.

[170] G. H. Sun, S. L. Yan, and G. Chen, "Analytical Model of Thermal Stress for Encapsulation and Service Process of Solar Cell Module," *Adv. Mater. Res.*, vol. 97–101, pp. 2699–2702, 2010.

[171] S. Dietrich, M. Pander, M. Sander, U. Zeller, and M. Ebert, "Stress analysis of encapsulated solar cells by means of superposition of thermal and mechanical stresses," *in SPIE - Reliability of Photovoltaic Cells, Modules, Components, and Systems V*, vol. 8825. San Diego, CA, USA, p.

882505, 2013.

[172] L. Yixian and A. A. O. Tay, "Finite element thermal stress analysis of a solar photovoltaic module," *in 37th IEEE Photovoltaic Specialists Conference*. Seattle, WA, USA, pp. 003179–003184, 2011.

[173] T. van Amstel, V. A. Popovich, and I. J. Bennett, "A Multiscale Model of the Aluminium Layer at the Rear Side of a Solar Cell," *in 24th European Photovoltaic Solar Energy Conference and Exhibition*. Hamburg, Germany, 2009.

[174] J. Dong, H. Yang, X. Lu, H. Zhang, and J. Peng, "Comparative Study on Static and Dynamic Analyses of an Ultra-thin Double-Glazing PV Module Based on FEM," *Energy Procedia*, vol. 75, pp. 343–348, 2015.

[175] A. Kilikevičius, A. Čereška, and K. Kilikevičienė, "Analysis of external dynamic loads influence to photovoltaic module structural performance," *Eng. Fail. Anal.*, vol. 66, no. Supplement C, pp. 445–454, 2016.

[176] M. Paggi and J. Reinoso, "Revisiting the problem of a crack impinging on an interface:A modeling framework for the interaction between the phase field approach for brittle fracture and the interface cohesive zone model," *Comput. Methods Appl. Mech. Eng.*, vol. 321, pp. 145–172, 2017.

[177] M. Paggi, M. Corrado, and M. A. Rodriguez, "A multi-physics and multi-scale numerical approach to microcracking and power-loss in photovoltaic modules," *Compos. Struct.*, vol. 95, pp. 630–638, 2013.

[178] M. Paggi, M. Corrado, and I. Berardone, "A global/local approach for the prediction of the electric response of cracked solar cells in photovoltaic modules under the action of mechanical loads," *Eng. Fract. Mech.*, vol. 168, pp. 40–57, 2016.

[179] A. Sapora and M. Paggi, "A coupled cohesive zone model for transient analysis of thermoelastic interface debonding," *Comput. Mech.*, vol. 53, no. 4, pp. 845–857, 2014.

[180] I. Berardone, M. Corrado, and M. Paggi, "A Generalized Electric Model for Mono and Polycrystalline Silicon in the Presence of Cracks and Random Defects," *Energy Procedia*, vol. 55, pp. 22–29, 2014.

[181] O. Breitenstein and S. Rißland, "A two-diode model regarding the distributed series resistance," *Sol. Energy Mater. Sol. Cells*, vol. 110, pp. 77–86, 2013.

[182] C. Buerhop *et al.*, "Evolution of cell cracks in PV-modules under field and laboratory conditions," *Prog. Photovoltaics Res. Appl.*, vol. 26, no. 4, pp. 261–272, 2018.

[183] J. H Wohlgemuth, D. W Cunningham, D. Amin, J. Shaner, Z. Xia, and J. Miller, "Using Accelerated Tests and Field Data to Predict Module Reliability and Lifetime," *in 23rd European Photovoltaic Solar Energy Conference and Exhibition*. Valencia, Spain, pp. 2663–2669, 2008.

[184] A. Bouraiou *et al.*, "Experimental investigation of observed defects in crystalline silicon PV modules under outdoor hot dry climatic conditions in Algeria," *Sol. Energy*, vol. 159, pp. 475–487, 2018.

[185] S. S. Chandel, M. Nagaraju Naik, V. Sharma, and R. Chandel, "Degradation analysis of 28 year field exposed mono-c-Si photovoltaic modules of a direct coupled solar water pumping system in western Himalayan region of India," *Renew. Energy*, vol. 78, pp. 193–202, 2015.

[186] V. Sharma and S. S. Chandel, "A novel study for determining early life degradation of multi-crystalline-silicon photovoltaic modules observed in western Himalayan Indian climatic

conditions," *Sol. Energy*, vol. 134, pp. 32–44, 2016.

[187] A. Dolara, S. Leva, G. Manzolini, and E. Ogliari, "Investigation on Performance Decay on Photovoltaic Modules: Snail Trails and Cell Microcracks," *IEEE J. Photovoltaics*, vol. 4, no. 5, pp. 1204–1211, 2014.

[188] I. Paul, B. Majeed, K. Razeeb, and J. Barton, "Statistical fracture modelling of silicon with varying thickness," *Acta Mater.*, vol. 54, no. 15, pp. 3991–4000, 2006.

[189] O. Borrero-López, T. Vodenitcharova, M. Hoffman, and A. J. Leo, "Fracture Strength of Polycrystalline Silicon Wafers for the Photovoltaic Industry," *J. Am. Ceram. Soc.*, vol. 92, no. 11, pp. 2713–2717, 2009.

[190] S. Schoenfelder, M. Ebert, C. Landesberger, K. Bock, and J. Bagdahn, "Investigations of the influence of dicing techniques on the strength properties of thin silicon," *Microelectron. Reliab.*, vol. 47, no. 2–3, pp. 168–178, 2007.

[191] M. Trautmann, M. Hemsendorf, C. Berge, C. Probst, and E. Rueland, "Non-contact microcrack detection from as-cut wafer to finished solar," *in 38th IEEE Photovoltaic Specialists Conference*. Austin, TX, USA, pp. 000485–000488, 2012.

[192] H. Behnken, M. Apel, and D. Franke, "Simulation of mechanical stress during bending tests for crystalline wafers," *in 3rd World Conference onPhotovoltaic Energy Conversion*, vol. 2. Osaka, Japan, pp. 1308–1311, 2003.

[193] J. Barredo, V. Parra, I. Guerrero, A. Fraile, and L. Hermanns, "On the mechanical strength of monocrystalline, multicrystalline and quasi-monocrystalline silicon wafers: A four-line bending test study," *Prog. Photovoltaics Res. Appl.*, vol. 22, no. 12, pp. 1204–1212, 2014.

[194] S. Schoenfelder, A. Bohne, and B. J., "Comparison of test methods for strength characterization of thin solar wafers," *in 22nd European Photovoltaic Solar Energy Conference and Exhibition*. Milan, Italy, pp. 1636–1640, 2007.

[195] T. Hauck, C. Bohm, and W. H. Müller, "Weibull statistics for multiple flaw distributions and its application in silicon fracture prediction," *in 6th International Conference on Thermal, Mechanical and Multi-Physics Simulation and Experiments in Micro-Electronics and Micro-Systems*, vol. 2005. Berlin, Germany, pp. 242–247, 2005.

[196] C. Bohm, T. Hauck, W. H. Muller, and A. Juritza, "Probability of silicon fracture in molded packages [ICs]," *in 5th International Conference on Thermal and Mechanical Simulation and Experiments in Microelectronics and Microsystems*. Brussels, Belgium, pp. 75–81, 2004.

[197] C. Bohm, T. Hauck, A. Juritza, and W. Mueller, "Weibull statistics of silicon die fracture," *Pm&r*. pp. 782–786, 2005.

[198] V. A. Popovich, M. Janssen, I. M. Richardson, T. van Amstel, and I. J. Bennett, "Microstructure and mechanical properties of aluminum back contact layers," *Sol. Energy Mater. Sol. Cells*, vol. 95, no. 1, pp. 93–96, 2011.

[199] V. A. Popovich, A. Yunus, M. Janssen, I. J. Bennett, and I. M. Richardson, "Effect of Microstructure and Processing Parameters on Mechanical Strength of Multicrystalline Silicon Solar Cells," *Sol. Energy Mater. Sol. Cells*, vol. 95, no. 1, pp. 2222–2226, 2010.

[200] J. G. Coletti, C.J.J. Tool and L. Geerligs, "Quantifying surface damage by measuring mechanical strength of silicon wafers," in *20th European Photovoltaic Solar Energy Conference and Exhibition*, 2005.

[201] K. Wasmer *et al.*, "Effects of edge defects induced by multi-wire sawing on the wafer strength," *in 23rd European Photovoltaic Solar Energy Conference and Exhibition*. Valencia, Spain, pp. 1305–1310, 2008.

[202] P. F. A. Schneider, E. Rueland, A. Kraenzl, "Mechanical and electrical characterisation of thin multi-crystalline silicon solar cells," *in 19th European Photovoltaic Solar Energy Conference*. Paris, France, pp. 496–499, 2004.

[203] C. Klute, F. Kaule, and S. Schoenfelder, "Breakage Root Cause Analysis in as-Cut Monocrystalline Silicon Wafers," *in 29th European Photovoltaic Solar Energy Conference and Exhibition*. Amsterdam, Netherlands, pp. 753–756, 2014.

[204] V. A. Popovich, A. Yunus, M. Janssen, I. M. Richardson, and I. J. Bennett, "Effect of silicon solar cell processing parameters and crystallinity on mechanical strength," *Sol. Energy Mater. Sol. Cells*, vol. 95, no. 1, pp. 97–100, 2011.

[205] V. A. Popovich, M. Janssen, I. J. Benett, and I. M. Richardson, "Breakage issues in silicon solar wafers and cells," *Photovoltaics Int.*, vol. 12, pp. 49–57, 2011.

[206] V. A. Popovich, W. Geerstma, M. Janssen, I. J. Bennett, and I. M. Richardson, "Mechanical Strength of Silicon Solar Wafers Characterized by Ring-On-Ring Test in Combination with Digital Image Correlation," *EPD Congress 2015*. Cham, pp. 241–248, 2015.

[207] F. Kaule, W. Wang, and S. Schoenfelder, "Modeling and testing the mechanical strength of solar cells," *Sol. Energy Mater. Sol. Cells*, vol. 120, no. Part A, pp. 441–447, 2014.

[208] V. Popovich, A. Yunus, M. Janssen, I. Bennett, and I. Richardson, "Mechanical strength of multicrystalline silicon solar cells and influencing factors," in *25th European Photovoltaic Solar Energy Conference and Exhibition*, 2010, pp. 2631–2636.

[209] C. Kohn *et al.*, "Influence of the metallization process on the strength of silicon solar cells," *in 24th European Photovoltaic Solar Energy Conference*. Hamburg, Germany, pp. 1419–1423, 2009.

[210] M. Sander, S. Dietrich, M. Pander, M. Ebert, and J. Bagdahn, "Systematic investigation of cracks in encapsulated solar cells after mechanical loading," *Sol. Energy Mater. Sol. Cells*, vol. 111, no. Supplement C, pp. 82–89, 2013.

[211] *IEC 61646. Thin-film terrestrial photovoltaic (PV) modules e design qualification and type approval*. International Electrotechnical Commission (IEC), 2008.

[212] G. Mülhöfer, H. Berg, C. Ferrara, W. Grzesik, and D. Philipp, "Influence of Mechanical Load at Low Temperatures on Cell Defects and Power Degradation at Full Scale PV Modules," *in 28th European Photovoltaic Solar Energy Conference and Exhibition*. Paris, France, pp. 2968–2971, 2013.

[213] C. Borri, M. Gagliardi, and M. Paggi, "Fatigue crack growth in Silicon solar cells and hysteretic behaviour of busbars," *Sol. Energy Mater. Sol. Cells*, vol. 181, pp. 21–29, 2018.

[214] V. Novickij, V. Višniakov, A. Kilikevičius, J. Novickij, A. Grainys, and P. Zapolskis, "Investigation of the Influence of the Dynamic Mechanical Loads on the Crystalline Structure of Photovoltaic Cells," *in 9th International Measurement conference*. Smolenice, Slovakia, pp. 179–182, 2013.

[215] S. Koch, J. Kupke, D. Tornow, M. Schoppa, S. Krauter, and P. Grunow, "Dynamic mechanical load tests on crystalline silicon modules," *in 25th European Photovoltaic Solar Energy Conference and Exhibition / 5th World Conference on Photovoltaic Energy Conversion*. Valencia, Spain, pp. 3998–4001, 2010.

1445 [216] M. Chang, C. H. Hsueh, H. Chen, and C. Chen, "Evaluating the influence of typhoon on PV module
1446 reliability," *32nd European Photovoltaic Solar Energy Conference and Exhibition*. Munich,
1447 Germany, pp. 2248–2251, 2016.

1448 [217] N. C. Dong, M. A. Islam, Y. Ishikawa, and Y. Uraoka, "The influence of sodium ions decorated
1449 micro-cracks on the evolution of potential induced degradation in p-type crystalline silicon solar
1450 cells," *Sol. Energy*, vol. 174, pp. 1–6, 2018.

1451 [218] O. Breitenstein, J. P. Rakotoniaina, M. H. Al Rifai, and M. Werner, "Shunt types in crystalline
1452 silicon solar cells," *Prog. Photovoltaics Res. Appl.*, vol. 12, no. 7, pp. 529–538, 2004.

1453 [219] O. Breitenstein, J. Bauer, P. P. Altermatt, and K. Ramspeck, "Influence of Defects on Solar Cell
1454 Characteristics," *Solid State Phenom.*, vol. 156–158, pp. 1–10, 2009.

1455 [220] J. Käsewieter, F. Haase, M. H. Larrodé, and M. Köntges, "Cracks in Solar Cell Metallization
1456 Leading to Module Power Loss under Mechanical Loads," *Energy Procedia*, vol. 55, pp. 469–477,
1457 2014.

1458 [221] M. Demant, T. Welschehold, S. Kluska, and S. Rein, "Microcracks in Silicon Wafers II:
1459 Implications on Solar Cell Characteristics, Statistics and Physical Origin," *IEEE J. Photovoltaics*,
1460 vol. 6, no. 1, pp. 136–144, 2016.

1461 [222] P. Hacke *et al.*, "Test-to-Failure of crystalline silicon modules," *in 35th IEEE Photovoltaic*
1462 *Specialists Conference*. Honolulu, HI, USA, pp. 244–250, 2010.

1463 [223] A. F. Dethlefsen, "Multi-crystalline silicon solar cell modules: crack formation and development
1464 due to climate chamber thermal cycle testing," in *Photovoltaic Module Reliability Workshop*, 2011.

1465 [224] O. Gonzalez, B. Diaz-Herrera, B. Gonzalez-Diaz, S. Gonzalez-Perez, L. Votta, and R. Guerrero-
1466 Lemus, "Forensic analysis of Si-based PV module micro-cracking due to standard IEC thermal and
1467 mechanical testing procedures," *in 43rd IEEE Photovoltaic Specialists Conference*. Portland, OR,
1468 USA, pp. 3041–3045, 2016.

1469 [225] D. Philipp, "PV module reliability and quality testing," *PV Investors Day*, pp. 1–22, 2015.

1470 [226] J. Lincoln *et al.*, "Forecasting Environmental Degradation Power Loss in Solar Panels with a
1471 Predictive Crack Opening Test," *in 44th IEEE Photovoltaic Specialist Conference*. 2017.

1472 [227] P. Grunow, P. Clemens, V. Hoffmann, B. Litzenburger, and L. Podlowski, "Influence of micro
1473 cracks in multi-crystalline silicon solar cells on the reliability of PV modules," *in 20th European*
1474 *Photovoltaic Solar Energy Conference and Exhibition*. Barcelona, Spain, pp. 2380–2383, 2005.

1475 [228] J. Wendt, M. Träger, M. Mette, A. Pfennig, and B. Jaeckel, "The link between mechanical stress
1476 induced by soldering and micro damages in silicon solar cells," *in 24th European Photovoltaic Solar*
1477 *Energy Conference*. Hamburg, Germany, pp. 3420–3423, 2009.

1478 [229] C. Camus, A. Adegbenro, J. Ermer, V. Suryaprakash, J. Hauch, and C. J. Brabec, "Influence of pre-
1479 existing damages on the degradation behavior of crystalline silicon photovoltaic modules," *J.*
1480 *Renew. Sustain. Energy*, vol. 10, no. 2, pp. 1–16, 2018.

1481

Highlights:

- The origin of cracks and the factors that affect them are explained in detail.
- A classification of cracks based on their characteristics is presented.
- An overview of experimental and numerical studies on cell cracks is conducted.
- The effect of cracks on the electrical characteristics of PV modules is debatable.
- The prediction and quantification of their long-term impact is not known yet.